University of Stavanger

Faculty of Science and Technology

MASTER'S THESIS

Study program/ Specialization: MSc Petroleum Engineering / Reservoir Engineering	Spring semester, 2015 Open access
Writer: Mahmoud S M Alaassar	…… (Writer's signature)
Faculty supervisor: Associate Professor, Hans Kleppe External supervisor(s): Senior Research Engineer, Anton Shchipanov	
Thesis title: Simulation and Interpretation of Well Tests in Pressure (Stress) Sensitive Reservoirs with Induced Fractures	
Credits (ECTS): 30	
Key words: Pressure dependent permeability Stress sensitive reservoirs Well testing Induce fracture Eclipse Saphir	Pages: ……46…… + enclosure: ..6… Stavanger, …15/06/2015…….. Date/year

Simulation & Interpretation of Well Tests in Pressure (Stress) Sensitive Reservoirs with Induced Fractures

Master Thesis

By

Mahmoud Alaassar

Supervisor:

Senior Research Engineer
Anton Shchipanov

Supervisor:

Associate Professor
Hans Kleppe

IRIS

International Research Institute
Stavanger

Universitetet i Stavanger

Faculty of Engineering and Science
University of Stavanger

Summary

In the petroleum industry pressure (stress) dependent permeability is usually not considered in reservoir simulations. It's often due to lack of laboratory and field data, which determines the level of pressure (stress) dependency. Neglecting pressure (stress) dependency in a reservoir model may cause troubles in history matching and reduce forecast capability. This study focuses on numerical simulation of well test responses for pressure (stress) sensitive formations and interpretation of these responses with analytical models. The goal is to show the value of conventional well testing theory in estimating characteristics of stress-sensitive reservoirs.

Generally, a stress-sensitive reservoir may be addressed in coupled simulation of fluid flow and geomechanics where the reservoir properties i.e. permeability are considered as stress-dependent. However, in a conventional reservoir simulation workflow (only fluid flow) these properties may be considered as pressure-dependent. In principle, permeability is a function of effective stress, but in practice a function of pressure may be used as a simplifying assumption. The thesis investigates dynamic permeability change as a function of pressure in stress-sensitive reservoirs using a conventional reservoir model. The simulations include hydraulic fracture and non-fractured formation. Induced fractures have a strong impact on fluid flow in formations, governing flow paths and sweep efficiency. It was assumed that the numerical simulations provide synthetic well test responses that represent real pressure measurements from a field.

Analytical solutions based on the permeability modulus concept have been suggested in the literature to analyze pressure transient tests in pressure (stress) sensitive reservoirs. This concept is also widely used to approximate results of laboratory studies. Using the concept of permeability modulus, the study presents numerical simulations for pressure sensitive reservoirs. Pressure transients with impact of permeability modulus, fractures and outer boundary effects have been numerically studied in detail. A step-rate test in an aquifer was numerically simulated to assist in determining the pressure dependent permeability. The numerical well test responses obtained with constant and pressure dependent permeability were combined with the analytical model responses generated by the well-test software where single-phase flow and constant reservoir properties are assumed.

Finally, the synthetic step rate test response resulted from numerical simulation of pressure sensitive reservoir was interpreted step-by-step using analytical models conventionally used in pressure transient analysis. The possibility to estimate correct permeability dependence on pressure using the analytical step-by-step interpretation was confirmed. It was shown that the pressure dependent permeability curve (permeability modulus) may be constructed from the interpreted permeability values. Therefore, this step-by-step interpretation approach may be used to estimate pressure dependent permeability for pressure (stress) sensitive reservoirs from actual field data.

Acknowledgements

Firstly, I would like to express my appreciation to my supervisor at IRIS, Senior Research Engineer Anton Shchipanov for providing me with such an interesting topic for my thesis. I thank him for his guidance with sharing his relevant studies and knowledge on this subject. His patience and encouragement have been an inspiration.

Special thanks goes to my supervisor at the University of Stavanger, Associate Professor Hans Kleppe for his great assistance and advice whenever needed. I also wish to thank the rest of the faculty in the petroleum department for their contributions to my academic achievements.

I would also like to give my appreciation to my brother, Ahmad for his help and support. And to my friends for their motivation when I needed it most.

Finally, my deepest and most sincere gratitude to my loving parents who helped me realize my potential and who inspired and encouraged me to strive academically.

Table of Contents

List of Figures

List of Tables

1 Introduction

In the petroleum industry permeability is usually considered as a constant value in reservoir simulations. On the contrary, permeability is sensitive to pressure (stress) changes, as laboratory core experiments demonstrated permeability dependence on stress. The presence of fractures makes the formation more deformable and sensitive to stress. In this thesis we present simulation cases where permeability is considered to be a function of pressure.

To improve the efficiency of reservoir modeling and forecasts, pressure dependent permeability ought to be included. This helps in gaining a better understanding of reservoir behavior and achieving more realistic well tests analysis. In this study we would like to evaluate capabilities and accuracy of conventional pressure transient analysis when the reservoir permeability is pressure dependent. This thesis investigates pressure (stress) sensitive reservoirs with complementary effect of induced fractures.

1.1 Objectives

In the study we employ a combination of analytical and numerical simulation tools to use Pressure Transient Analysis (PTA) in characterizing pressure- (or more generally stress-) sensitive reservoirs where general objectives are:

- Numerical simulation of well tests in pressure-sensitive reservoirs;
- Effect of induced fractures in the simulation of well tests.
- Analysis of capabilities of analytical models to interpret pressure dependent permeability from the well test data.

1.2 Scope of Work

According to the objectives the study may be divided into the following tasks:

- Setting up segment reservoir models with a single well with possibility to account for pressure-dependent permeability using the Eclipse reservoir simulator.
- Simulation of well tests consisting of flowing and shut-in periods, i.e. bottom-hole pressure transients at specified rates.
- Analysis of specific behavior of the pressure transients governed by the pressure-sensitive permeability.
- Setting up analytical models with constant reservoir permeability in the Saphir PTA tool to match uploaded results from equivalent Eclipse simulations (to get the numerical simulations in line with the analytical models).
- Analysis of capabilities of the analytical (PTA) methods to interpret pressure dependent permeability from the pressure transients, e.g. through analysis of step-rate tests with multiple pressure transients.

2 Theory of Well Testing

Well testing is based on the concept of sending a signal to the formation around the wellbore in the reservoir and receiving its response. The data from this response is used to evaluate the well conditions and reservoir characteristics around the wellbore and distances to boundaries.

The influence in well testing may reach up to 500 meters. The large area of analysis allows to estimate reservoir permeability, porosity, initial and average pressure, fracture length, heterogeneities, distances to the different boundaries, and other conditions as well. These data contribute in the production analysis model (i.e. well test models), which are designed to be a predictive model. The predictive model helps engineers to simulate the production forecast of the reservoir and run different scenarios for production.

In the reservoir, fluid flows at different times in diverse ways based on the setting (size, shape, pressure variation with time) of the reservoir. There are three main flow regimes: they are steady state flow, pseudo-steady state flow and transient state flow.

Well Flowing Period

Pressure drawdown period corresponds to flowing production well conditions, which gives better results when the pressure in the formation is equalized, to reach this condition the well may be shut before the test. It is thus recommended to perform the test on new wells where the reservoir has uniform pressure. The test measures the bottom-hole pressure (through down-hole gauges) in the wellbore during a period of constant production rate (constant flow). A drawdown test is usually performed to back up the buildup test results to minimize uncertain interpretations.

Well Shut-in Period

Prior to pressure buildup period a constant production for a period of time may occur. The buildup period then starts by stopping the production and shutting the wellhead to build pressure in the well. During both the flowing and the shut-in periods bottom-hole pressure is measured and this is used for analysis.

2.1 Pressure Transient Analysis

Pressure transient analysis (PTA) is interpretation of pressure change in the well (the reservoir sand face or well-head) over a certain period of time. The reservoir characteristics together with data from PTA are applied to a mathematical model. The region around the well would always dominate the drawdown and buildup pressure transient behavior, the depth of this region depends on the well if it's intersecting fractures or not.

Pressure transient analysis is used to diagnose flow regimes and estimate well and reservoir parameters. The PTA is considered as one of the main sources of reservoir data. The methodology is standard but doesn't provide a unique solution. The quality of interpretations may be improved by availability of accurate and more frequent pressure data from electronic pressure gauges (i.e. down-hole), also advanced computer software greatly aids in the interpreting process. Pressure recorded at constant rate using down-hole pressure gauges is considered the most suitable data to use in the interpretation. Flow regimes if present may be identified using pressure transient data. But there is still need to improve the interpretation models and techniques to achieve more accurate results to present a better understanding of the reservoir and how it changes during field production.

Pressure transient analysis in oil and gas reservoirs with dynamic reservoir characteristics is quiet challenging where reservoir characteristics are assumed to be dependent on pressure (stress) i.e. porosity and permeability. Therefore with pressure changing in the reservoir due to production/injection these characteristics are harder to be determined.

2.1.1 Transient-, Pseudo-Steady- and Steady- State Flow

Transient state flow exists for a short period due to pressure disturbance in the reservoir. This state flow occurs at early times after flowing period and at early times after a shut-in period. When the pressure at the wellbore changes, the fluids in the reservoir will start to flow near the well expanding the pressure change which provokes flow further in the reservoir's undisturbed region. The pressure response during transient flow is not influenced by the outer boundary of the reservoir (size of the reservoir), i.e. infinite-acting reservoir is assumed.

The pressure distribution through the reservoir is determined by the fluid and reservoir characteristics, i.e. permeability and heterogeneity, until boundary effects are reached then steady- or pseudo-steady- state is seen. Therefore, transient flow response is important in well test interpretation.

When the pressure response reaches the outer boundary, two states may be observed. For the steady-state flow the pressure gradient over time is zero, i.e. pressure does not decline at the boundary, this is known as constant pressure boundary. In a pseudo-steady-state (PSS)

the pressure gradient over time is constant, i.e. pressure drop is uniform throughout the reservoir this is known as no flow boundary (closed system).

The terms above are used to describe flow from a well at constant flow rate. The reservoir flow phases are shown in Figure 2.1.

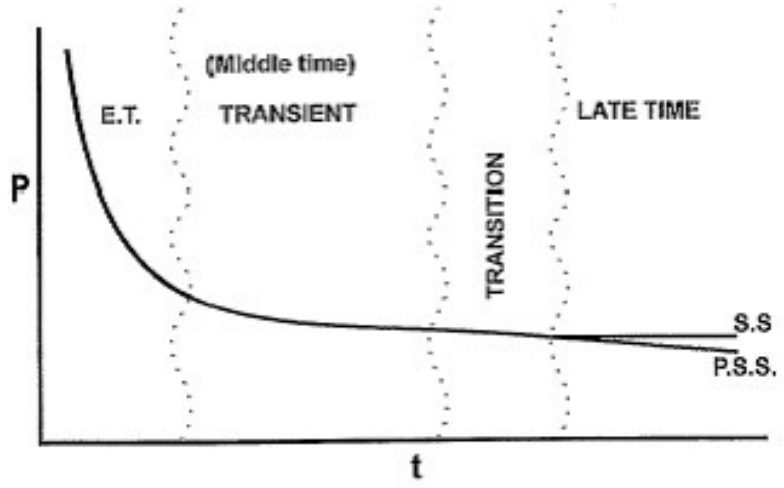

Figure 2.1: Flow regimes (www.fekete.com)

A reservoir with very low permeability may be in a transient flow phase for a long time before stabilizing in pseudo-steady-state regime. The formation linear flow or bi-linear (fracture flow) regime could also be observed in this flow phase. With reference to simulation, a very large grid block size (coarse) may mask the transient state flow, and then the pseudo-steady state is observed early.

2.1.2 Outer Boundary Conditions

This section presents how to identify the boundary effects. The outer boundary effect is the late time regime that appears after the infinite-acting period ends when the pressure response reaches a boundary (i.e. fault) or the reservoir limit (finite reservoir). The two most common boundary regimes are:

- No flow boundary
- Constant pressure boundary

No flow boundary (closed system) behavior is characteristic of limited reservoirs and in reservoirs where several wells are producing and each well drains a certain volume of the reservoir (Matthews and Russell, 1967).

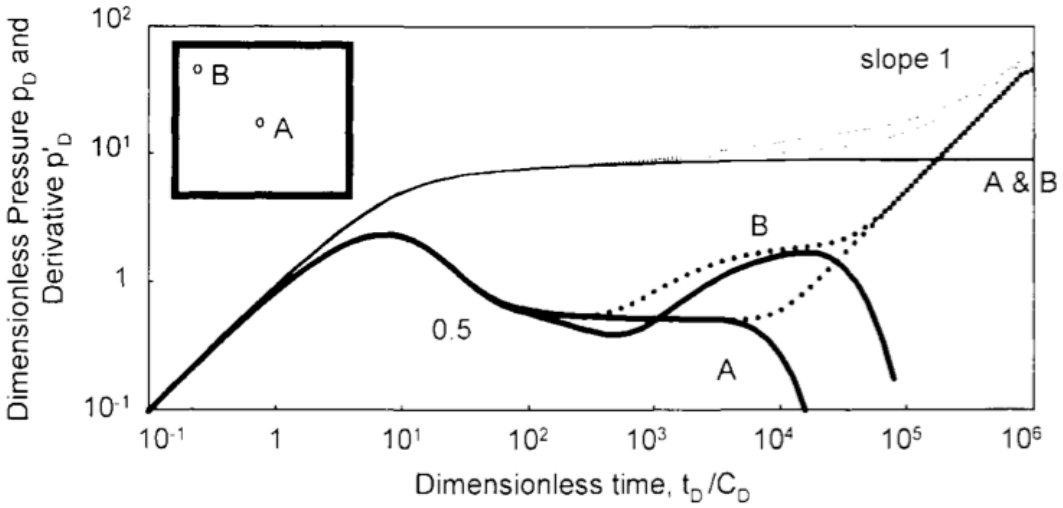

Figure 2.2: Pressure & derivative response for two wells in a closed square reservoir (dotted curve - drawdown, line - buildup). (Bourdet, 2002)

The boundary effects at late times may give different curve shapes in a log-log plot (pressure change and pressure derivative curves) for flowing and shut-in periods. For a closed reservoir system, PSS flow regime can only be observed from the flowing period represented by a straight-line unity slope. However, after the shut-in period pressure stabilizes and goes towards an average reservoir pressure causing a different well response for the same boundary condition.

For a constant pressure boundary, during both the flowing and shut-in periods the pressure stabilizes and the derivative goes towards zero following a straight line with negative unit slope. Here the rate of decline indicates the geometry of the boundary.

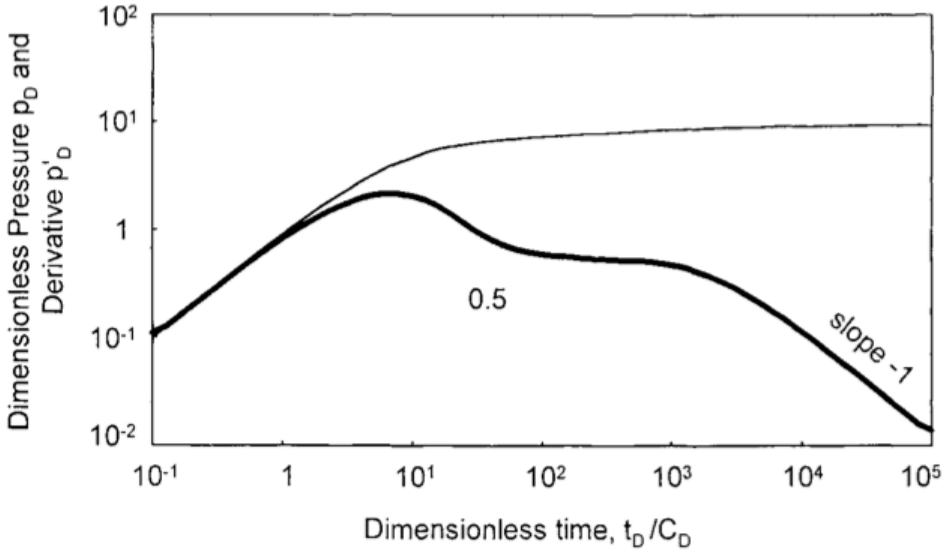

Figure 2.3: Pressure & derivative response for a well near a constant pressure boundary. (Bourdet, 2002)

When several constant pressure boundaries are reached, the shape of the response becomes close to that of a build-up curve in a bounded (closed) system (Bourdet, 2002).

2.2 Hydraulic Fractures

Hydraulic fracturing is an effective stimulation treatment implemented in low permeability reservoirs to increase the flow rate of hydrocarbons and increase the drainage area in the formation. Normally the fractures are generated vertically through the perforations in the well. How the fluid flows towards a single vertical induced fracture is shown below (Figure 2.4).

The main flow regimes that may occur around a vertical hydraulic fracture are the fracture linear flow, the formation linear flow and the pseudo-radial flow. At very early times, the fracture linear flow is the first flow period that exists but for a short period and might be concealed by the wellbore storage (flow comes from inside the fracture).

At slightly later times, the bilinear flow occurs, where fluid flows linearly towards the fracture and from the fracture to the well, this flow period forms in finite-conductivity fractures only (usually long fractures or natural fractures). Whereas the formation linear flow (also known as linear flow) forms to infinite-conductivity fractures. The linear flow can be considered as the most important flow regime during production.

After a long flow period, the fracture appears to be part of the wellbore and therefore a radial flow is observed after all flow regimes, its known as pseudo-radial flow.

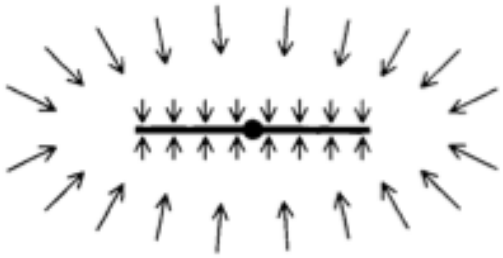

Figure 2.4: Linear and Pseudo-radial flow regimes, infinite conductive fracture. (Bourdet, 2002)

2.2.1 Infinite Conductivity Fracture

Cinco and Samaniego (1981) suggested three transient flow models to be accounted for in well testing of hydraulically fractured formation:

- Infinite conductivity vertical fractures
- Finite-conductivity vertical fractures
- Uniform-flux fractures

In a finite conductivity fracture the conductivity profile is high near the wellbore and becomes low as it goes deeper in the reservoir (changing pressure drop). Whereas for an infinite conductivity fracture the fluid flows in the fracture with uniform pressure i.e. pressure drop along the fracture is negligible. A uniform flux has a slight pressure gradient that corresponds to a uniform distributed flux.

In section 2.2 it was noted that at an early time the formation linear flow occurs in infinite conductive fractures only, the flow in this regime is perpendicular to the fracture surface. Later, during the transition period from the linear flow regime to the radial flow regime an elliptical flow shape forms (Figure 2.4).

The uniform flux fracture model is similar to the infinite conductivity fracture. The flow rate from the formation into fracture is uniform through the entire length, but is distinguished at the fracture boundaries. As seen from the figure 2.5 below, the linear and pseudo-radial flow regimes are similar for both models yet differ for the transition period.

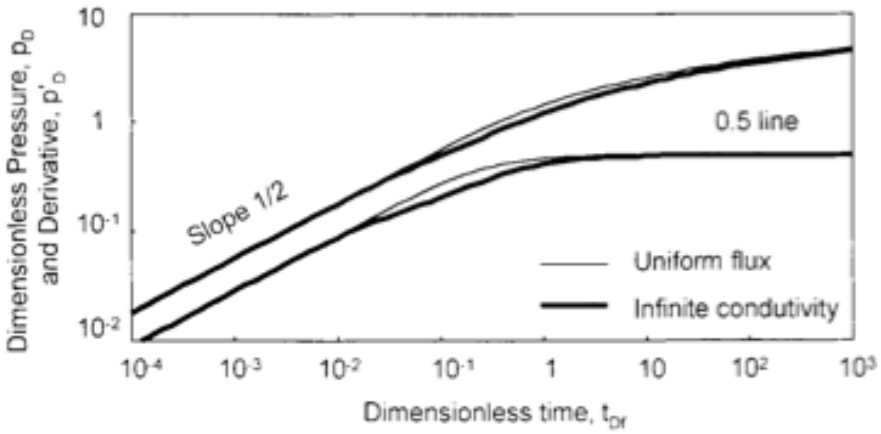

Figure 2.5: Infinite conductivity and uniform flow models for well intercepting a fracture (Bourdet, 2002)

The main two flow regimes are analyzed as such:

- A half-unit slope straight line for the pressure and derivative in the log-log plot identifies linear flow regime.
- A semi-log straight line identifies the pseudo-radial flow regime. This flow regime provides the permeability thickness product (kh).

2.2.2 Linear Flow in Tight Formations with Fracture

The linear flow regime is observed in oil and gas reservoirs, where it can be associated with flow to induced hydraulic fractures. As an example a vertical well with an infinite-conductivity fracture extending vertically from the well to the boundary of a linear tight oil reservoir may be considered (Figure 2.6). Here, infinite-conductivity is presumed for the hydraulic fracture so that oil flow to the well and oil flow to the fracture are equal. When the well is producing with constant bottom-hole pressure, the fracture surface serves as a constant pressure boundary for the linear system. While production continues under this condition, the pressure disturbance moves away from the fracture and production rate decreases. When the pressure disturbance reaches the outer boundary the flow period ends.

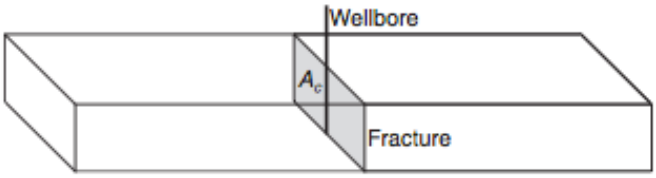

Figure 2.6: Linear reservoir with hydraulic fracture (SPE 162741-PA)

In the fracture the pressure is constant since the permeability of the fracture is very high. Linear fracture flow occurs to the hydraulic fracture since the conductivity is infinite.

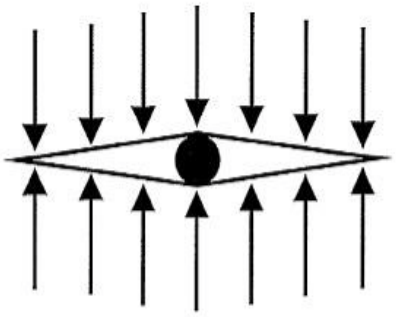

Figure 2.7: Linear flow towards fracture

The flow equation for the above system is a nonlinear partial differential equation (PDE) where permeability and porosity are assumed to be exponential functions of pressure.

$$\frac{\partial}{\partial x}\left(\frac{k}{\mu_o B_o}\frac{\partial p}{\partial x}\right) = \frac{\emptyset\, c_t}{B_o}\frac{\partial p}{\partial t} \qquad (1)$$

2.3 Stress Sensitive Formation

The properties of rock are pressure- or more generally stress-sensitive to a certain degree. In many cases description of transient fluid flows in porous media are based on the assumption of constant rock properties. But such description is not necessarily applicable to reservoirs where significant changes occur in rock properties due to variations in pore pressure. Based on the effective stress law, fluid withdrawal from reservoirs lowers pore pressure and causes an increase in effective stress.

In tight formations (low permeability) and fractured rock systems the permeability may be very sensitive to pore pressure change. The decrease in pore pressure leads to an increase in effective stress and following as a result to reductions in permeability (conductivity) and total porosity.

2.3.1 Pressure Dependent Permeability

Normally permeability is assumed to be constant in well test analysis, however permeability may change with pressure as mentioned in the previous section. In some cases if pressure dependence of permeability is not taken into account then inaccurate or false values of permeability may be calculated from the well test analysis.

Al Hussainy et al. (1966) introduced a definition for real gas pseudo-pressure *m(p)*, which is commonly used for well test analysis:

$$m(p) = 2\int_{p_o}^{p} \frac{p}{\mu(p)z(p)}dp \tag{2}$$

This transformation variable is used in the derivation to linearize the flow terms, which allows the analysis to be implemented to gas flow from the liquid case. But since permeability is pressure dependent another variable is needed that takes into account that permeability is a function of pressure *k(p)*.

$$\ddot{m}(p) = 2\int_{p_m}^{p} \frac{k(p)p}{\mu(p)z(p)}dp \tag{3}$$

Raghavan et al. in (1972) worked on this problem and presented a special transformation (pseudo-pressure) to linearize the problem. They concluded that the *m(p)* function is excellent in linearizing constant mass- rate oil transient tests for all practical flow rates.

Samaniego et al. (1977) investigated the influences of pressure dependent fluid properties and stress-sensitive rock properties on pressure transient analysis. They presented the results investigating the application of the *m(p)* method to drawdown, buildup, and injection testing.

Kikani and Pedrosa (1991) presented the use of a regular perturbation technique to solve the nonlinear equation to the third order of accuracy. They investigated the first-order effects of wellbore-storage, skin, and boundary effects. They also suggested the use of the zero-order perturbation solution to investigate wellbore storage, skin and outer boundary effects on pressure transient responses for stress-sensitive reservoirs. An example was analyzed to determine the permeability modulus and reservoir properties.

To solve the nonlinear problem with pressure dependent permeability, the permeability modulus is defined in a similar way to how compressibility is defined i.e.:

$$\gamma_p = \frac{1}{k}\frac{dk}{dp} \tag{4}$$

Nur et al. 1985 introduced the permeability modulus parameter to study flow through stress dependent media (pressure dependent reservoirs). This parameter measures the dependency of permeability on pore pressure in tight formations and fractured rock systems.

$$k = k_i * e^{-\gamma_p(p_i - p)} \tag{5}$$

Equation 4 gives a particular variation of permeability on pressure, which is exponential and this relationship is shown in equation 5.

Raghavan and Chin (2004) suggested three correlations for stress sensitive reservoirs where the permeability reduction is based on experimental data. The correlations are in linear, exponential and power law form. In this thesis, the exponential pressure dependence parameter is used to model the stress (pressure) dependent permeability.

2.3.2 PTA for Pressure Sensitive Reservoirs

This section addresses the characteristics of the well testing responses for pressure (stress) sensitive reservoirs. The pressure transient analysis is presented for constant reservoir properties compared to pressure-dependent reservoir properties. During the well test period the pressure varies constantly providing the data for PTA in pressure sensitive reservoir. Furthermore, only permeability is a function of effective stress in the pressure-dependent case.

Knowledge of the pressure- (stress) permeability relationship is key in order to determine the impact of pressure sensitive permeability on the reservoir performance as well as improve the management of stress sensitive reservoirs. The data from well tests can provide evidence of pressure-dependent permeability.

The fundamental concept of PTA to determine pressure sensitive permeability depends on the semi-log straight-line slope. The change in permeability due to change of pressure in the reservoir alters the slope.

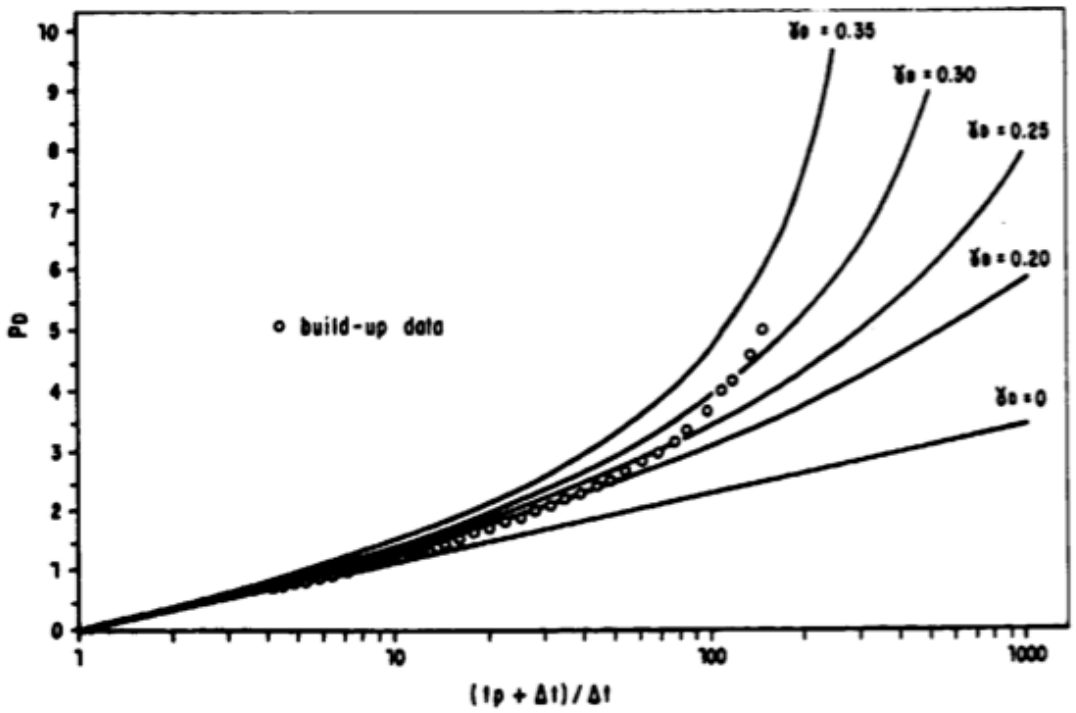

Figure 2.8: Buildup pressure behavior for a gas well in stress-sensitive reservoir (SPE 15115)

The figure above shows the semi-log plot for a buildup test in a gas well. The straight line below in the plot ($\gamma = 0$) represents the reservoir with constant properties. Moreover, the rest of the lines represent pressure-dependent properties with varying dependency of permeability on pressure.

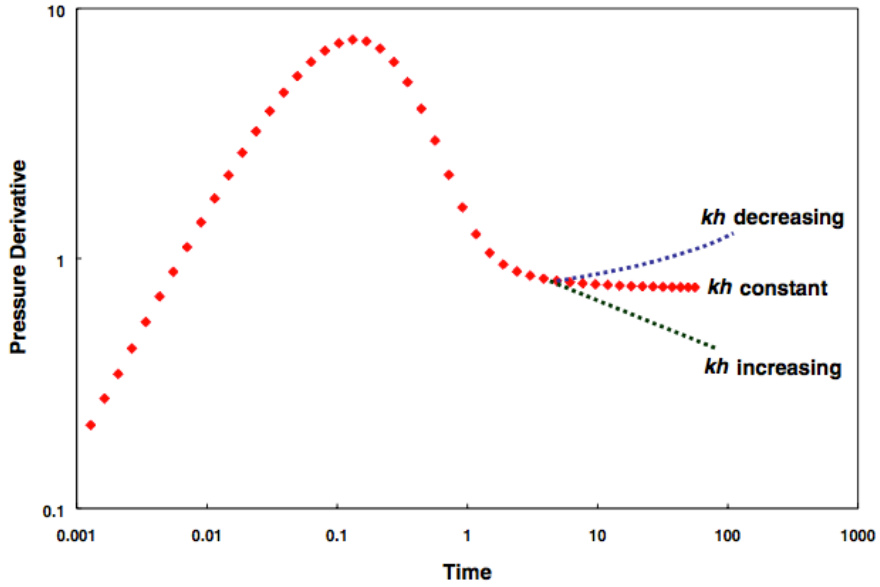

Figure 2.9: Permeability sensitivity in a pressure derivative plot (SPE 71034)

Pressure (logarithmic) derivatives are more sensitive to small effects than the conventional straight line and log-log analysis. The pressure derivative is very useful in identifying permeability variation. The radial flow line, represented by a straight horizontal line for constant permeability (flow capacity), may show different slopes for increasing/decreasing reservoir permeability.

Evidence of stress-sensitive permeability can be diagnosed by the following characteristics (Pinzon, 2001):

- Time- and Rate-dependent logarithmic derivatives of pressure transients
- Inconsistent results between drawdown and buildup analysis
- Unusual value of skin
- Rate-sensitive skin

Using analytical solutions Pedrosa (1986) and Samaniego et al. (2003) determined the characteristic behavior of pressure transients in the presence of pressure dependent permeability. This behavior of stress-sensitive reservoirs have been confirmed by coupled flow-geomechanics simulations (Chin et al., 2000).

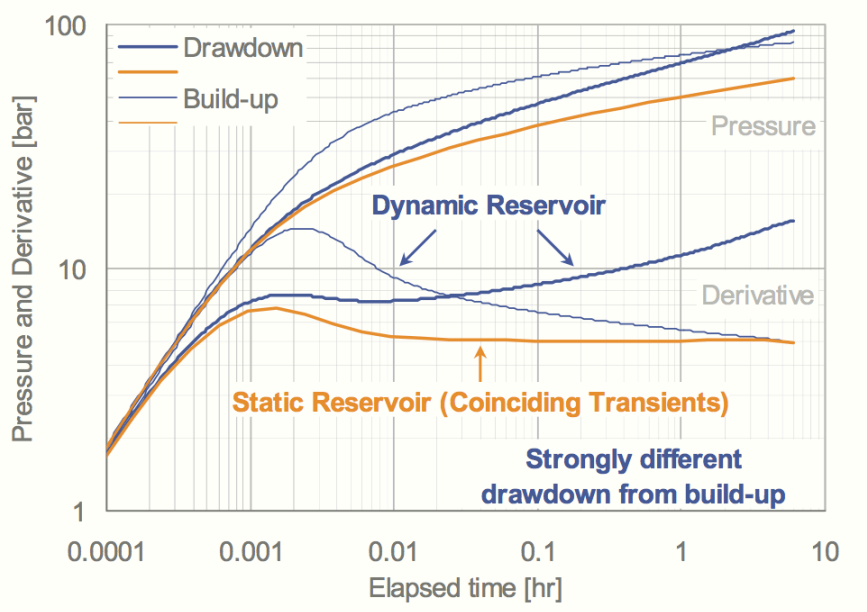

Figure 2.10: Dynamic permeability in synthetic drawdown & build-up pressure transients (Shchipanov et al, 2011)

Pressure (stress) sensitivity of reservoirs and fractures causes changes in permeability and porosity. The non-linear pressure diffusivity equation, where permeability is a function of pressure, is used to describe flow in these reservoirs. This has consequences on PTA, i.e. absence of infinite acting radial flow regime (IARF) and strong difference between drawdown and build-up derivatives (figure 2.10). Nonetheless, PTA is capable of interpreting pressure transients influenced by pressure dependent permeability.

3 Reservoir Simulation Studies

The main purpose for reservoir simulation is to evaluate the behavior of the reservoir under different production schemes to optimize and predict future forecasts. Reservoir simulators are programs for solving the reservoir flow equations.

Reservoir simulation is based on the construction and criteria's set to run the model with characteristics similar to the reservoir, so it can obtain representative and useful results to further develop and produce efficiently. The mathematical model used in a simulator is a group of differential equations, which under certain initial and boundary conditions describe the basic physical principles in a reservoir.

3.1 Single-phase Case Study

This section describes a scenario that allows us to get a better understanding of the impact of assuming constant permeability or/and pressure dependent permeability in the reservoir. A mechanistic reservoir model was developed to study the difference these different cases simulated.

The model represented a single homogeneous layer, filled with water containing an injection well centered in the aquifer. An induced hydraulic fracture is also considered as a case when the vertical well is stimulated. The aquifer has an area of 1000 m^2 with a thickness of 10 meters in the model. Eclipse Blackoil Reservoir Simulator (E100) is used for the simulations.

A well test consisting of an injection period (well flowing) with a constant rate of 50 sm3/day during 60 days (1440 hours), followed by a fall-off period (well shut-in) during the same test. The bottom-hole pressure is simulated at logarithmic time. The simulation results are analyzed using the log-log plot of the pressure and pressure derivative calculated for the different cases.

Reservoir data used in the well test simulation:

Grid	100*100*1
Wellbore radius	0,1 meters
Aquifer thickness	10 meters
Porosity	0,1
Viscosity of fluid (water)	1 cP
Total compressibility	0,0005 1/bars
Permeability	5 md
Initial reservoir pressure	400 bars
Injection rate	50 m3/day

Table 1: Reservoir Properties

To simulate pressure dependent permeability k(p) in the model, two keywords are used, the rock compaction option (ROCKCOMP) which allows us to implement pressure dependent pore volume and transmissibility multipliers as tables versus pressure (ROCKTAB). In this way dynamic reservoir parameters are achieved which are pressure (stress) dependent.

3.1.1 Simulation Case 1: Constant Permeability

In the first case, the model is simulated with the initial characteristics mentioned above, where there is no induced fracture assumed in this case and the permeability in the reservoir (matrix) is constant.

In both the injection and fall-off responses in Figure 3.1 the following is noticed. At early times, the pressure and derivative curves are overlying in a unit slope that represents the grid block storage mimicking the wellbore storage period. Since the reservoir has a low permeability reservoir (i.e. permeability for grid blocks) the duration of the wellbore period is longer, this is due to the water injected taking time to go from the well to the formation.

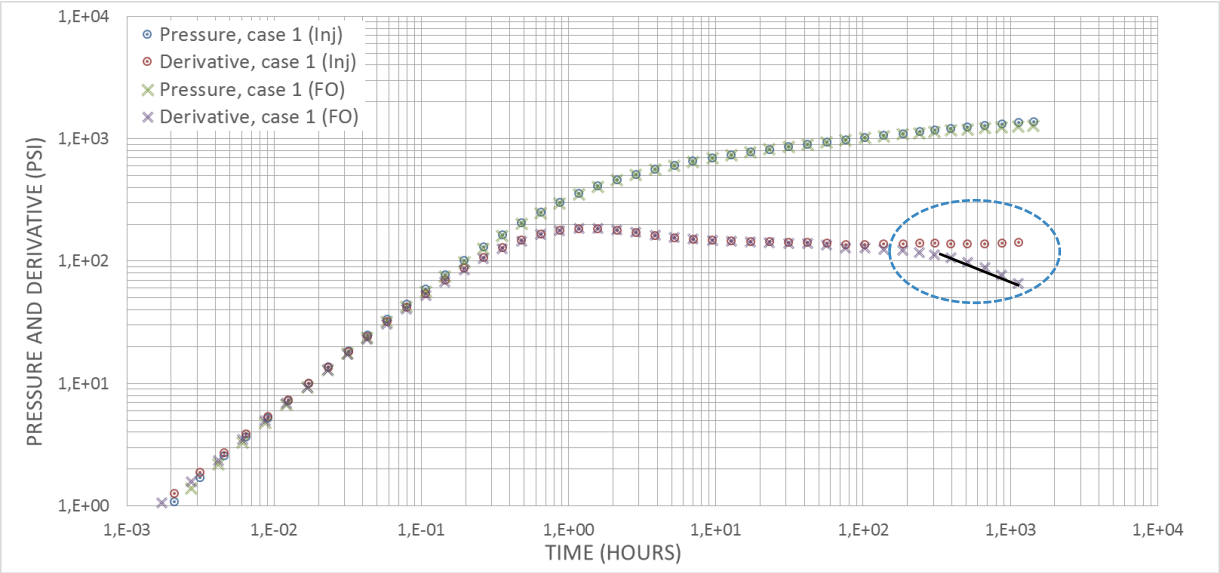

Figure 3.1: Pressure and derivative responses for Case 1 (no fracture, k=constant)

After the wellbore period, the pressure response comes from the reservoir. Following the transition period (plunge) the pressure derivative becomes constant shown by the flattening of the derivative on the log-log plot, this represents the radial flow period in the reservoir, while the pressure curve also shows that infinite acting radial flow period is reached. From the radial flow period the important reservoir parameters such as permeability can be estimated.

At late time, the boundary effects here are not observed (infinite reservoir/no boundary regime). After looking at the pressure response dynamics using a visualization software, it is clear that pressure change from the injection test has not reached to the boundaries of the reservoir. Therefore the boundary regime is not observed from the injection pressure derivative.

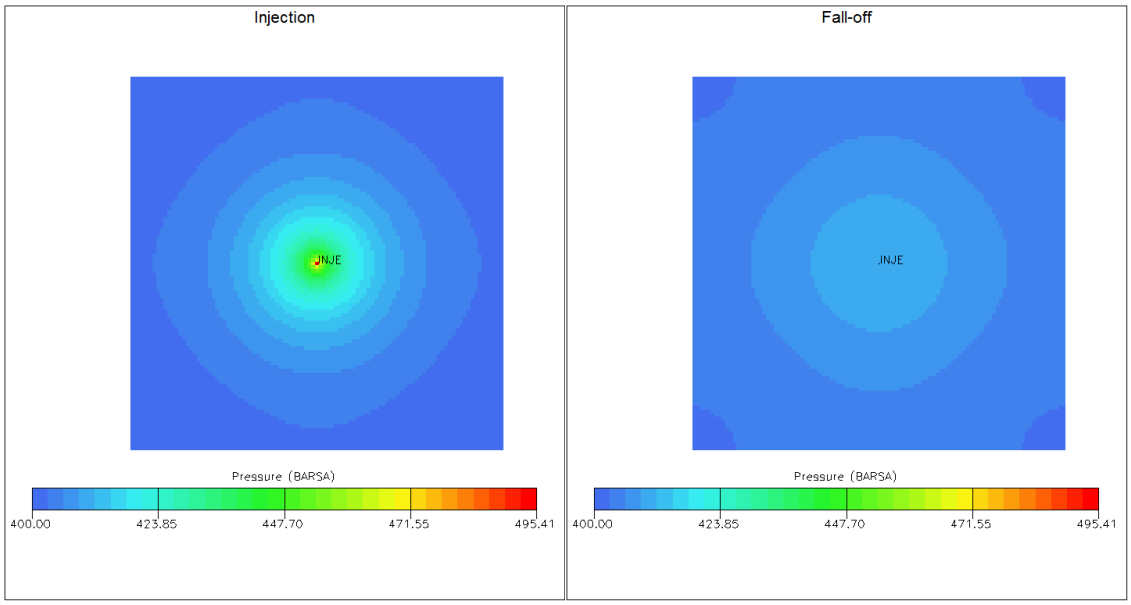

Figure 3.2: Pressure response of reservoir at the end of Injection & Fall-off (k=constant)

The fall-off derivative is showing a downward dip which may represent a negative unit slope that means the boundary i.e. reservoir limit is reached. In Figure 3.2, a comparison between the injection and fall-off pressure responses explains the curves on the log-log plot, here the pressure fall-off response reaches the boundary of the reservoir unlike the injection response.

3.1.2 Simulation Case 2: Constant Permeability with Fracture

In this case a hydraulic fracture is implemented in the model extending vertically from the well, by setting a high directional permeability in the same direction as the fracture (x-direction), this method helps to simulate a hydraulic fracture in an easy way. The length of the fracture is $1/10^{th}$ of the reservoir. A sensitivity study is simulated to see the impact of permeability on the fracture.

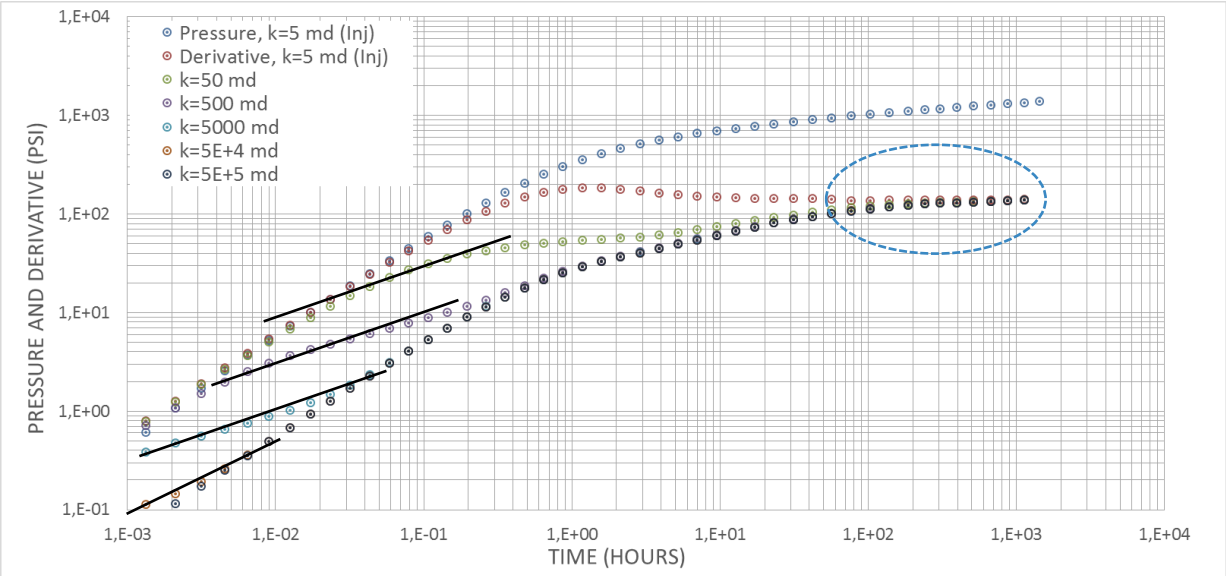

Figure 3.3: Pressure and derivative responses for Case 2. Sensitivity on fracture permeability.

The lines drawn in the log-log plot on the pressure derivative are quarter unit slope (¼) and half unit slope (½) lines, which represent the bilinear flow and the linear flow regime respectively. As the permeability increases, linear flow regime is shown earlier and becomes clearer, whereas the grid block storage period diminishes and is harder to observe on the plot. The bilinear flow occurs when the conductivity of the fracture is finite whereas linear flow regime represents infinite conductivity of the fracture.

At the end all the pressure derivatives stabilize and take the form of a horizontal straight line representing pseudo-radial flow regime, which is the similar regime to radial flow when no fracture is present. From the pseudo-radial flow regime the permeability thickness product (kh) can be calculated.

3.1.3 Simulation Case 3: Pressure Dependent Permeability

In this case there is no fracture in the matrix and pressure dependent permeability k(p) is implemented using the functions explained. Transmissibility is multiplied in x- and y-directions increasing with the increase in pressure. The pore volume, which is a function of the porosity and compressibility of the rock, also increases. Below are part of the values used under the ROCKTAB function to mimic k(p).

ROCKTAB				
Pressure	Pore Volume	Trans X-	Trans Y-	Trans Z-
300	0,95	0,37	0,37	1
350	0,98	0,61	0,61	1
400	1	1,00	1,00	1
450	1,03	1,65	1,65	1
500	1,05	2,72	2,72	1
550	1,08	4,48	4,48	1
600	1,11	7,39	7,39	1
650	1,13	12,18	12,18	1

Table 2: ROCKTAB keyword (pore volume and transmissibility multipliers)

Bottom-hole pressure versus time for the simulated model is presented (figure 3.4) using an output software. The results are imported to Excel (spreadsheet) for all the cases to help plot the pressure and derivative of each case.

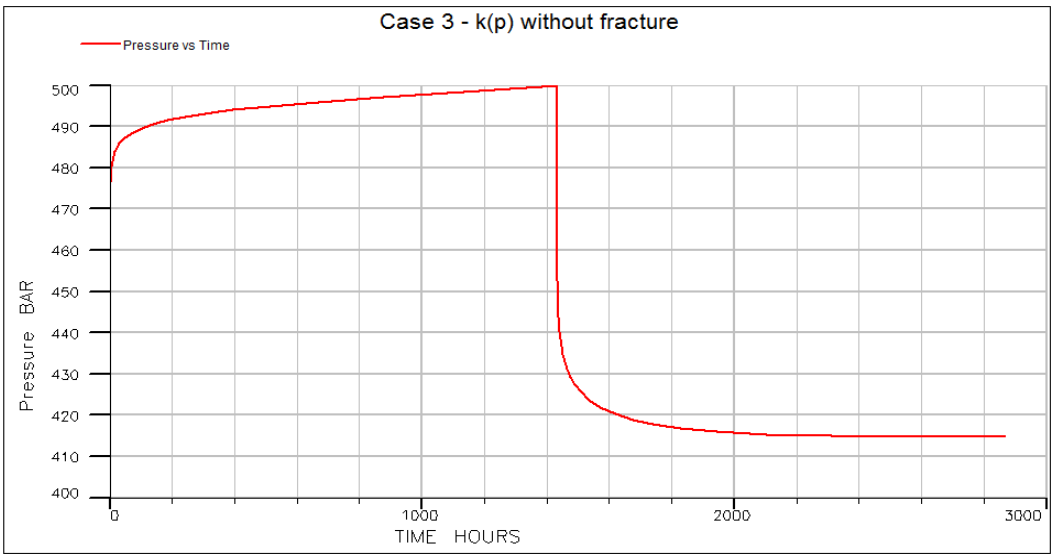

Figure 3.4: Pressure vs Time during injection & fall-off for Case 3

Below we show the pressure dependent permeability multiplier versus the pressure, k(p) plot (figure 3.5). The permeability modulus parameter ($\gamma = 0.01$) with Eq. 5 is used to calculate the permeability multiplier for all the cases with pressure sensitivity. Permeability increases exponentially with pressure, this is represented by transmissibility (table 2).

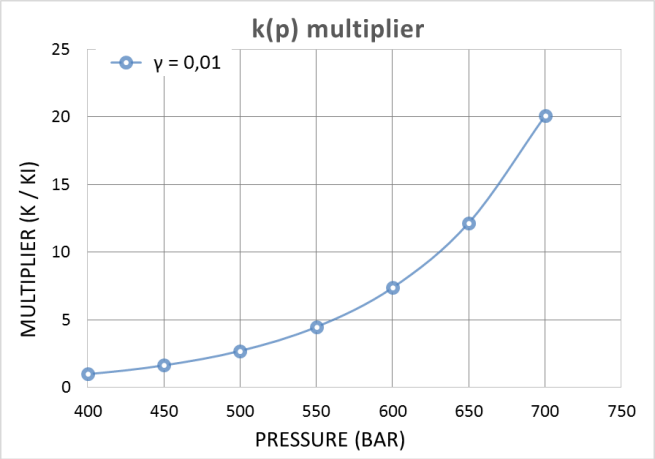

Figure 3.5: k(p) plot

Figure 3.6 shows the comparison of the pressure and pressure derivative curves where constant permeability is assumed for the reservoir (case 1) and when pressure dependent permeability is implemented (case 3). At early times, again the unit slope representing the grid block storage is shown, since in these cases hydraulic fracture is not assumed, the early flow regime is easily visible.

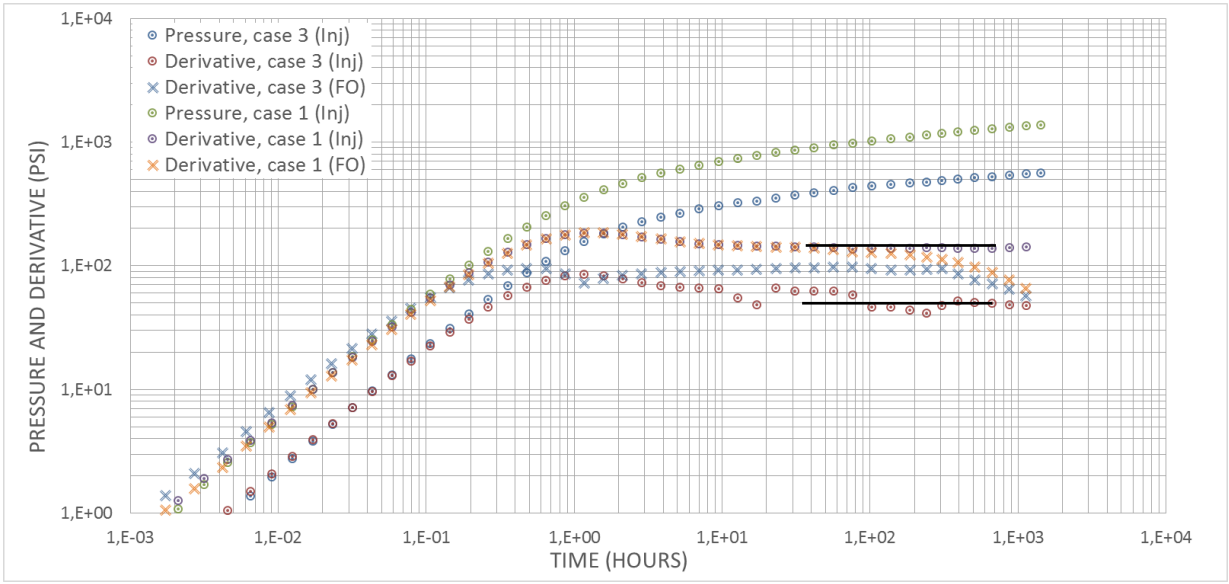

Figure 3.6: Comparison between pressure and derivative responses for Case 1 & Case 3 (k vs k(p), no fracture)

With pressure dependent permeability the reservoir achieves radial flow sooner than when permeability is constant. Also the radial flow regime shifts down (figure 3.6) when k(p) is implemented which means flow capacity has increased, hence the permeability increased.

At late times, the k(p) case and permeability constant case 1, reach the boundary of the reservoir with the same time. The boundary effect is only observed from the fall-off pressure derivatives, a straight-line slope meaning pseudo steady state regime is reached (closed system). For the rest of the cases where k(p) is implemented the closed system (no flow boundary) is observed from the pressure derivative of the fall-off test.

3.1.4 Simulation Case 4: Pressure Dependent Permeability with Fracture

In this case, the hydraulic induced fracture is implemented from the injector well and pressure dependent permeability is implemented in the matrix (reservoir) except the fracture (k=constant). This case is compared with case 2, where permeability is constant. The objective is to observe k=constant vs k(p) for the simulation model (reservoir), here represented by case 2 and case 4.

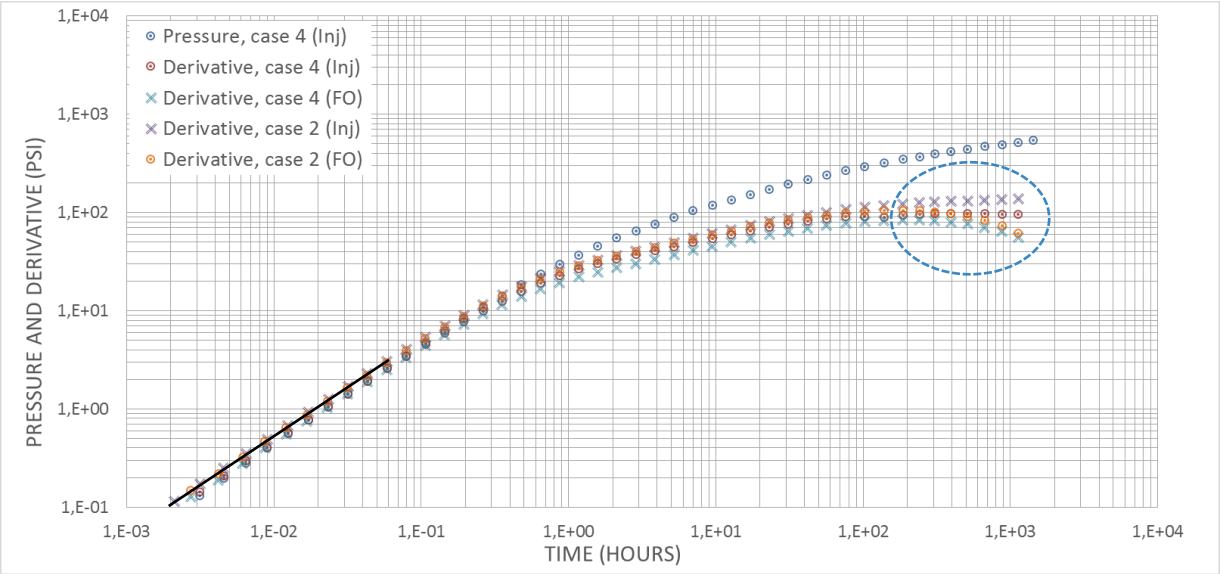

Figure 3.7: Comparison between pressure and derivative responses for Case 2 & Case 4 (k vs k(p), with fracture)

The half slope shows the linear flow regime early in the reservoir, which is better presented in both the pressure dependent permeability case and constant permeability.

The radial flow regime decreases slightly in pressure (stress) dependent permeability (case 4) compared to constant permeability, this represents flow capacity increase. This is better observed in the previous case, in the comparison of k=constant vs k(p) for the no fracture cases. The conclusion is that pressure dependent permeability leads to an increase in the reservoir flow capacity (kh) and this increase is much less in the presence of an induced fracture.

Below we observe the pressure change around the simulated hydraulic fracture when permeability is constant (case 2) and when permeability is pressure dependent (case 4). The comparison below shows a visualization of the pressure profile in both cases after injection is done (60 days). Here, the elliptical flow shape can be seen in red and yellow around the fracture, this flow geometry forms after the linear flow regime and before the radial flow behavior is reached. The shape of the pseudo-radial flow regime can be seen later as analyzed from the diagnostic plots.

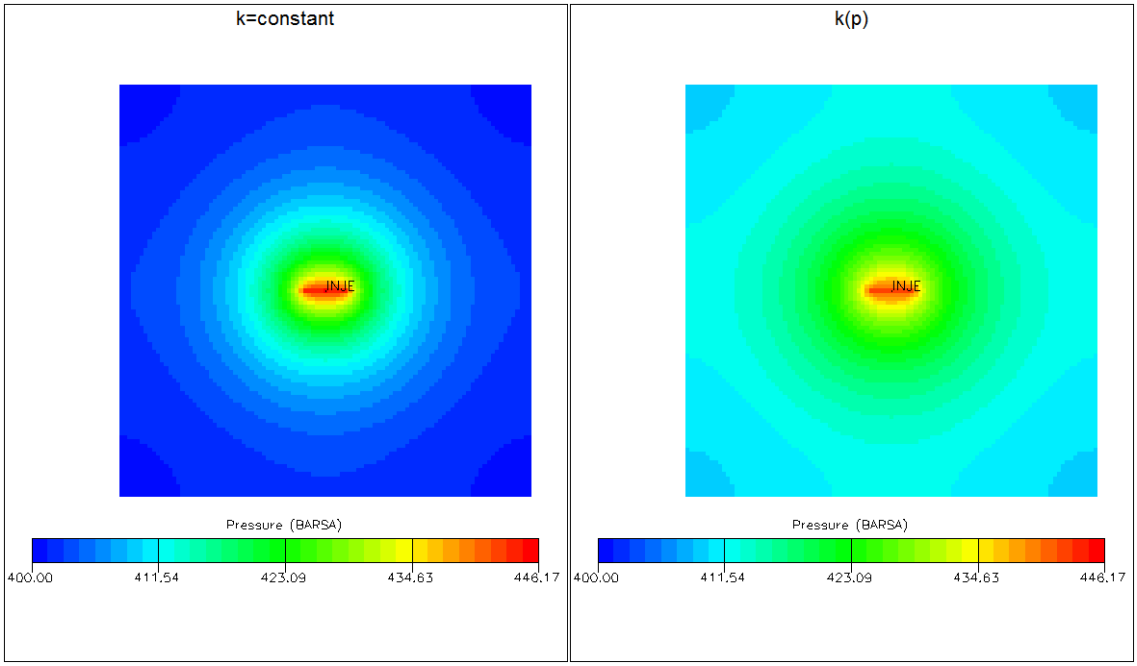

Figure 3.8: Pressure response of reservoir with induced fracture (k & k(p))

Two variations of Case 4

First variation, case 4.1 which is similar to case 4 with the exception of including the fracture with the pressure effects implemented on the matrix where permeability is pressure dependent. Permeability in the fracture and the matrix is now dependent on pressure. The purpose of simulating this case is to observe the effect of k=constant and k(p) on the fracture.

The second, in case 4.2 the roles change, permeability is assumed constant in the matrix. Whereas in the fracture, the permeability is dependent on pressure. This will help give a better understanding on the effect of k(p) and k=constant for the simulated reservoir strictly.

Comparing case 4 with case 4.1, it is clear that the pressure and pressure derivative curves match. This implies that as long as pressure dependent permeability is assumed in the matrix then it has the biggest impact on the pressure transient curves, and impact of k(p) in the fracture is negligible.

In pressure (stress) sensitive formation where permeability is assumed to be pressure dependent, wouldn't affect an infinitely conductive fracture. This is seen in Figure 3.9 below for the comparison between k=constant & k(p) in the fracture. The pressure and derivative curves overlap accurately for case 4 and case 4.1.

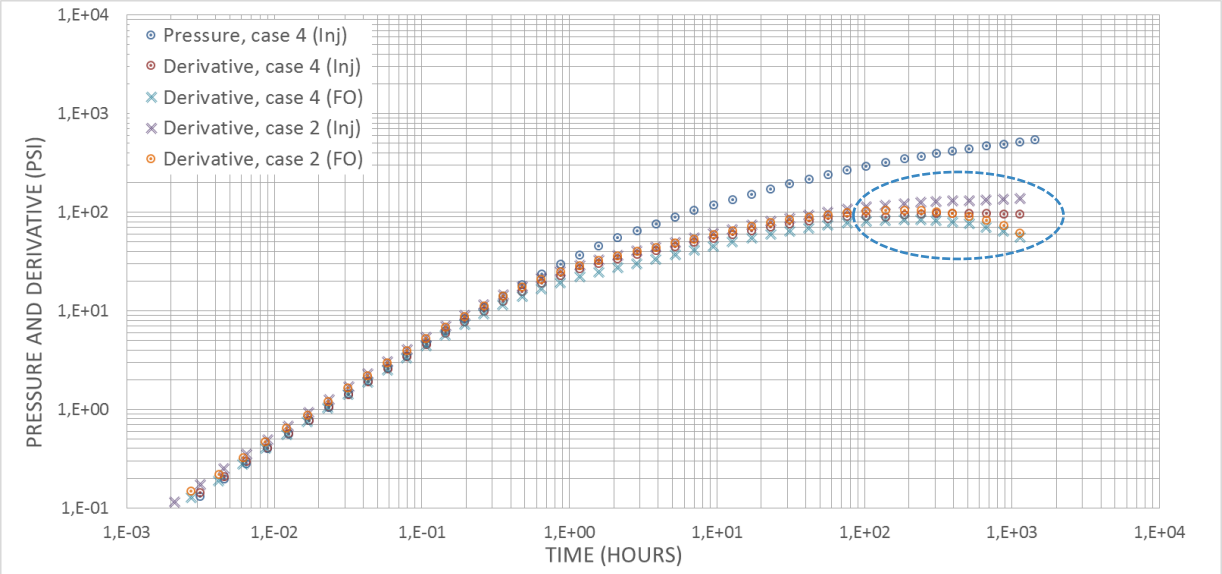

Figure 3.9: Comparison between pressure and derivative responses for Case 4, Case 4.1 & Case 4.2

Case 4.2 is compared with case 4, the first thing noticed is that the early time period matches perfectly now, hence the condition of the fracture (whether k(p) or k=constant) has no effect at early times. At later times, in the pseudo-radial flow period and boundary effect, the impact of k=constant versus k(p) on the reservoir (matrix) is visible, the pressure change is higher when k=constant and the pressure derivative during radial flow is also higher. The pseudo-radial flow shows that the permeability is retained (k=constant) as opposed to the case where the reservoir is under k(p) and permeability increases (flow capacity).

After studying the two variations of case 4 where comparison of k=constant vs. k(p) is done for the fracture and reservoir (matrix) separately, a clear picture is reached of the extent the impact k(p) has on an infinite conductivity fracture. The early time period and transition period are not affected by the impact of a pressure (stress) sensitive formation for an infinite conductive fracture. However, the pressure response further away from the fracture into the reservoir, has an impact on the flow capacity when k(p) is assumed for the reservoir.

3.2 Reservoir Property Sensitivities

3.2.1 Fracture Permeability Study

The purpose of this sensitivity is to help choose the fracture permeability where the fracture acts infinitely conductive. This is achieved when the pressure throughout the length of the fracture is uniform as noted in section 2.2.1. The plots below give a closer look on the pressure in the grid blocks that represent the fracture half-length (blocks 1-6). The hydraulic fracture extending with 5 grid blocks from each side and the well placed in the center. For the fracture to be infinitely conductive, the pressure in each block from the well to the end of the fracture should be equal.

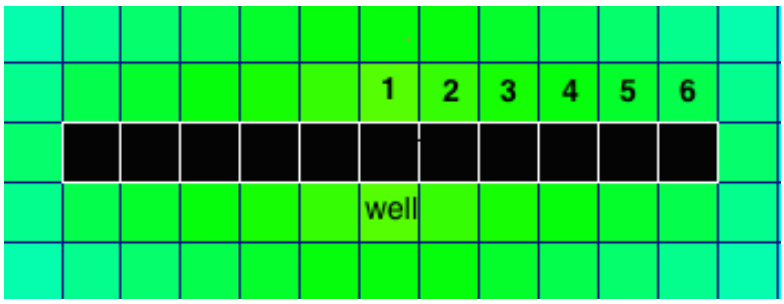

Figure 3.10: Grid blocks in the fracture

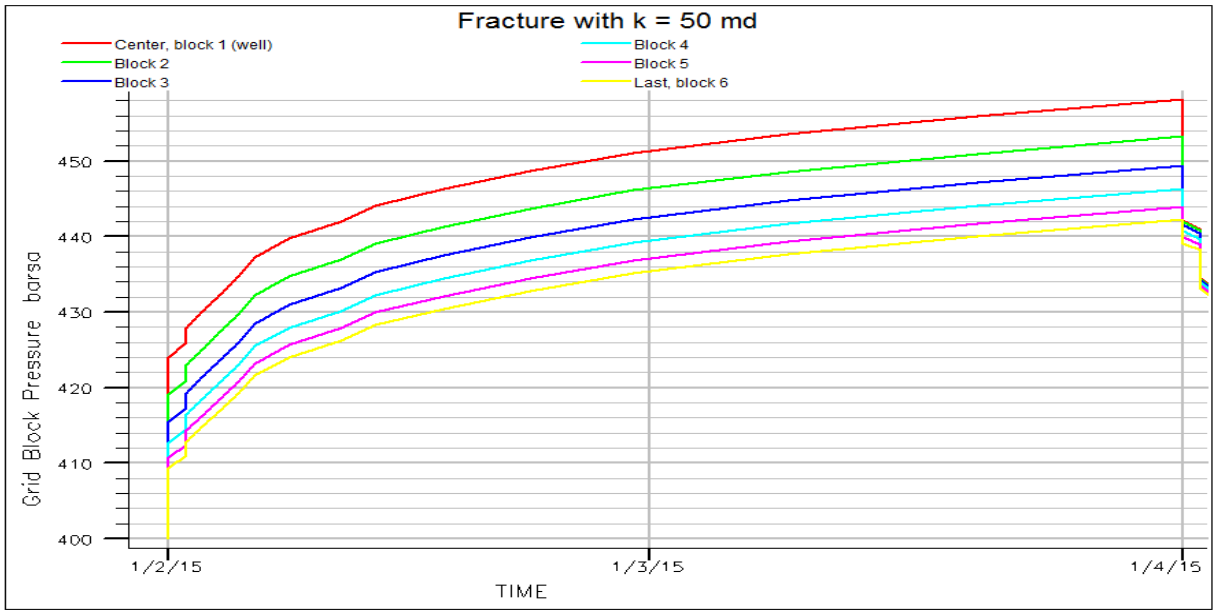

Figure 3.11: Grid block pressure for fracture with 50md permeability

The pressures in the grid blocks from the center (well) to the end of the fracture are plotted. Figure 3.11 shows that pressure is not equal throughout the fracture, meaning the fracture is finitely conductive. This changes when the permeability of the fracture increases to 5000md (thousand times the matrix). Here all the grid blocks have an almost equal pressure, therefore the criteria for infinite conductivity is achieved.

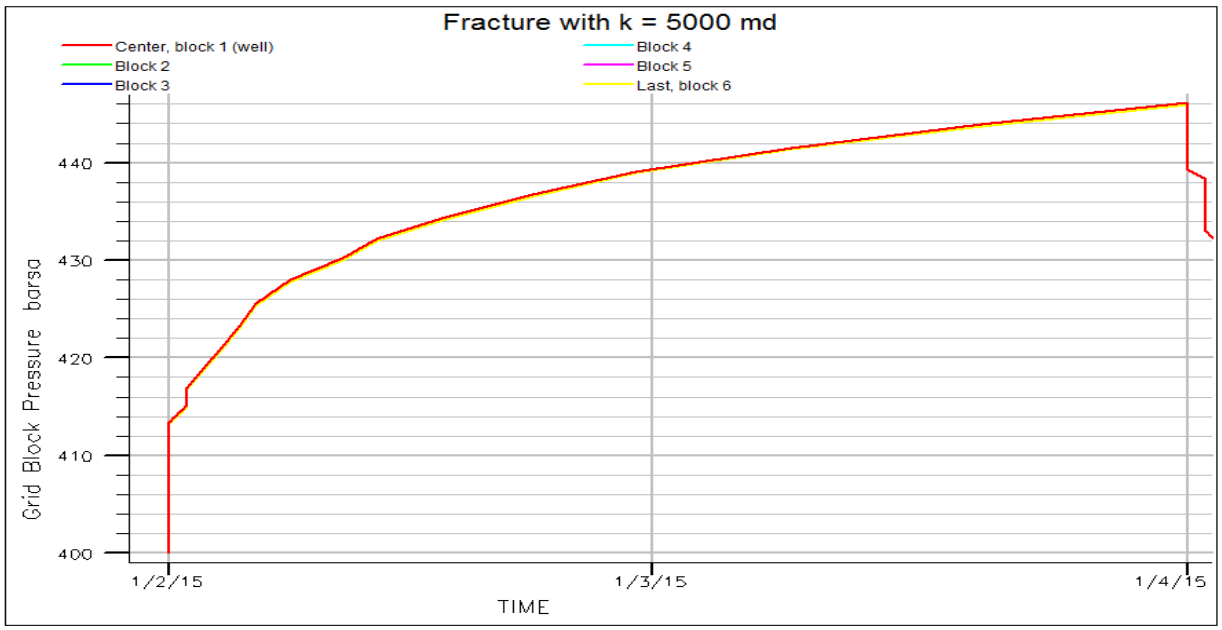

Figure 3.12: Grid block pressure for fracture with 5000md permeability

Based on figure 3.12, the fracture with permeability higher than 5000md would fulfill the criteria and may be assumed as infinitely conductive. Hence, to ensure that the fracture is infinitely conductive in the simulation cases, fracture permeability is taken to be 5.0E+5md.

3.2.2 Reservoir Size & Boundary Effects

Sensitivity is preformed on grid block size (reservoir size) to study the grid block storage effect on pressure and derivative curves. First, sensitivity was done for grid block size in z-direction (aquifer thickness), from the initial size of 10 meters to 50 meters. Here, increase in the thickness of the reservoir increases the flow capacity.

Second, another sensitivity was done for the grid block size in x- and y- directions. From Figure 3.13 below it is observed that even with the increase or decrease in the reservoir size the derivative curves converge to a constant flow capacity (kh), making the impact limited to the grid block storage effect that changes. When the grid block size is reduced from 10 to 5 meters the aquifer size is reduced, therefore the boundary effect is observed earlier.

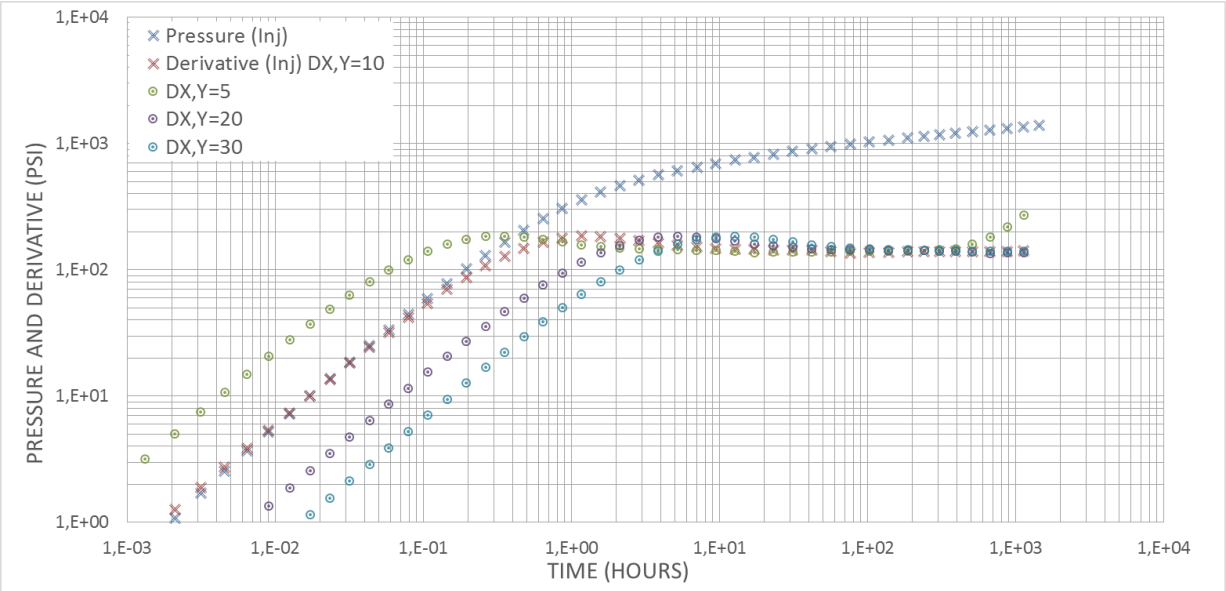

Figure 3.13: Pressure and derivative responses for Case 1. Sensitivity on grid block size in x- & y-directions.

After understanding the impact of the reservoir size on the derivative curves and how reducing the size can give an earlier boundary effect. The block size in all directions (x, y, z) is reduced ($1/5^{th}$ the area) in order to determine how different boundary effects are observed in the plot. The simulated model used in the cases above is assumed to have a no flow boundary (closed reservoir), for this boundary regime the derivative of injection and fall-off periods has different responses, an upward and a downward plunge. The boundary regime hasn't been clearly identified in the interpretation of the simulation cases.

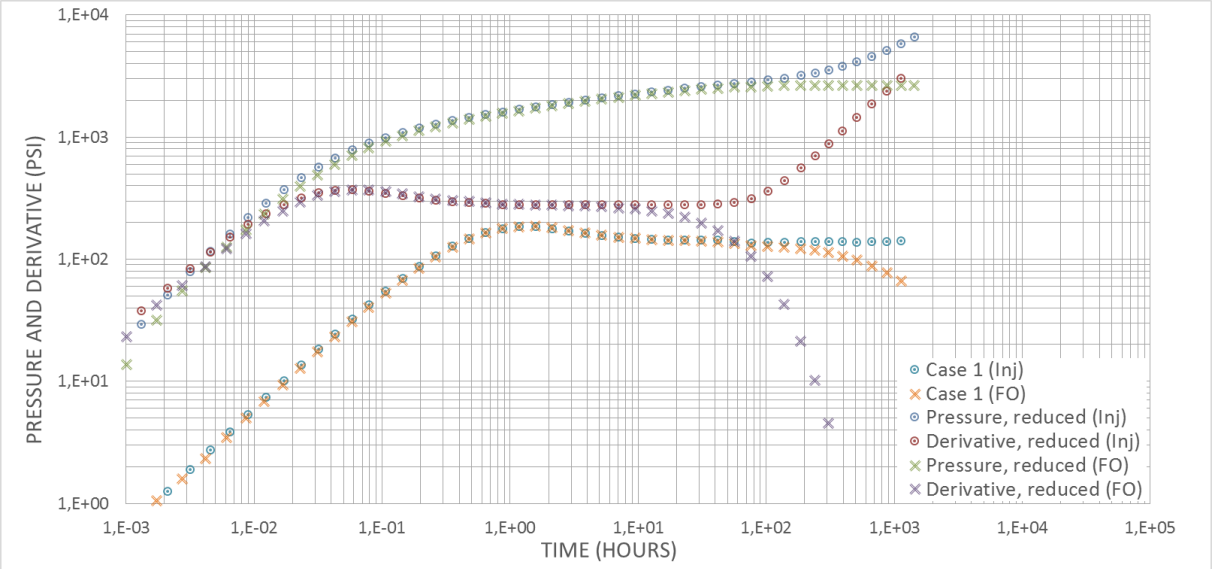

Figure 3.14: Pressure and derivative responses for Case 1. No Flow boundary.

The new pressure and derivative of the injection period at late time shows a pseudo steady state regime presented by an approaching straight line unity slope between both curves, while the fall-off period drops (figure 3.14). These two different responses confirm that we have a no flow boundary that was just not reached due to the size of the reservoir (grid block size). Now that the boundary regime from the simulation is identified as a no flow boundary, we implement constant pressure boundary in the simulated model (reservoir) by putting very high porosity in the boundary grid blocks and observe how the derivative curves changes to a straight line with negative unit slope (figure 3.15). The outer boundary effects observed were explained in section 2.1.2.

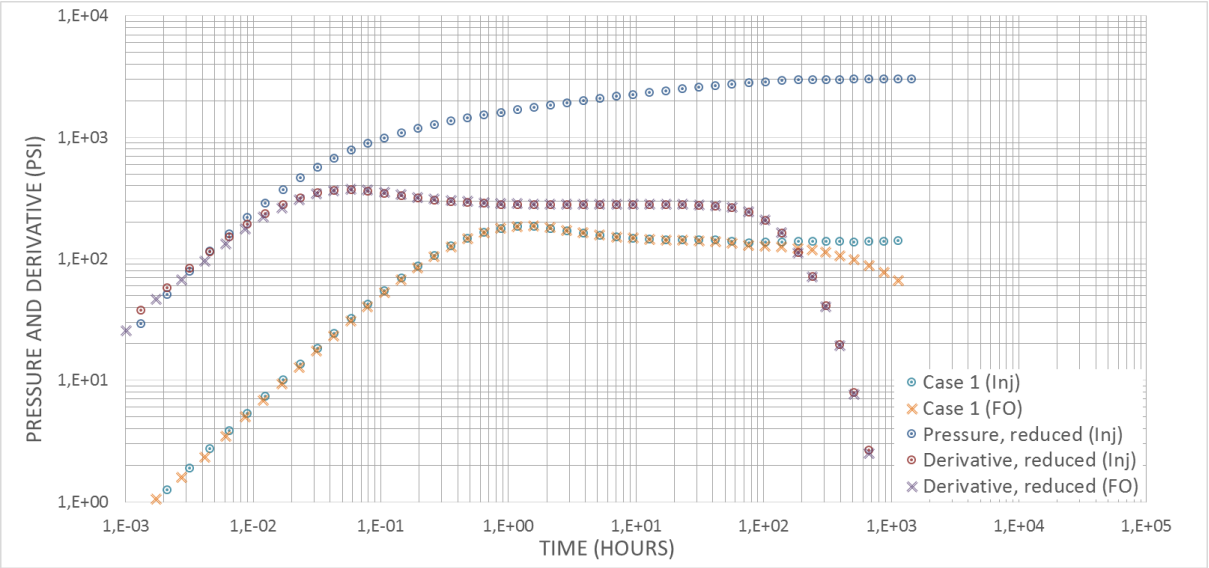

Figure 3.15: Pressure and derivative responses for Case 1. Constant Pressure boundary.

3.3 Conclusion of Simulation Studies

In this chapter we studied the impact of assuming constant permeability or pressure dependent permeability in the reservoir. Dynamic changes of reservoir parameters are achieved in the simulation by implementing certain options (please see section 3.1). The model developed helped simulate the cases and to analyze the results using log-log plots.

Based on the simulation cases, some interesting observations follow:

- The well block storage effect looks similar to the wellbore storage effect lasting for some time in beginning of a transient.
- Infinite conductivity effect (no impact of further conductivity increase on the results) is achieved with fracture permeability of 5000 md.
- Injection & fall-off responses are different for pressure dependent permeability from those obtained with constant permeability (figure 3.6 & 3.7).
- No flow boundary effect (closed system) is only observed from the fall-off period (figure 3.1, 3.6 & 3.7)
- Pressure derivative shifts down at k(p) with injection, which represents permeability increase at pressure build-up (figure 3.6 & 3.7)
- The induced fracture increases flow capacity near the wellbore decreasing the derivative shift when comparing k(p) vs. k = constant cases (figure 3.7).
- Pressure dependent permeability does not significantly affect the simulated linear fracture flow (figure3.8).

This chapter presented a simple way of interpreting flow regimes, flow boundaries, fracture effects and identifying pressure sensitive effects in log-log plots.

4 Combining Analytical & Numerical PTA

This chapter includes the pressure transient results of analytical model and numerical simulation of pressure dependent permeability using step-rate test. The analysis is presented for different flow regimes as well as constant injection rate in a number of increasing rates in order to estimate the permeability at different pressure periods. The base case model used in the simulation runs is included in Appendix A.

The numerical simulation results are presented by pressure and pressure derivative curves plotted using SAPHIR (PTA tool). We obtain the bottom-hole pressure values, the rates and time intervals from the simulation model runs using ECLIPSE. The PTA tool generates analytical models based on the well-reservoir parameters provided by ECLIPSE, which helps us interpret the results. The match between the analytical model and the numerical simulation may show that the interpretation gives the same well & reservoir parameters.

4.1 Constant Permeability

This section presents the numerical simulation from ECLIPSE and the analytical model from SAPHIR for Case 1 with constant permeability (section 3.1.1). The aim is to combine both the analytical and numerical solutions to show a good match in the PTA tool for the well-reservoir parameters used in ECLIPSE. This will be the starting point that we further use to match and interpret the step-rate test cases. The important point is to analyze the part of the pressure derivative curve that corresponds with transient flow, in order to estimate the permeability. This section will be the bases for combining the analytical-numerical method in further sections.

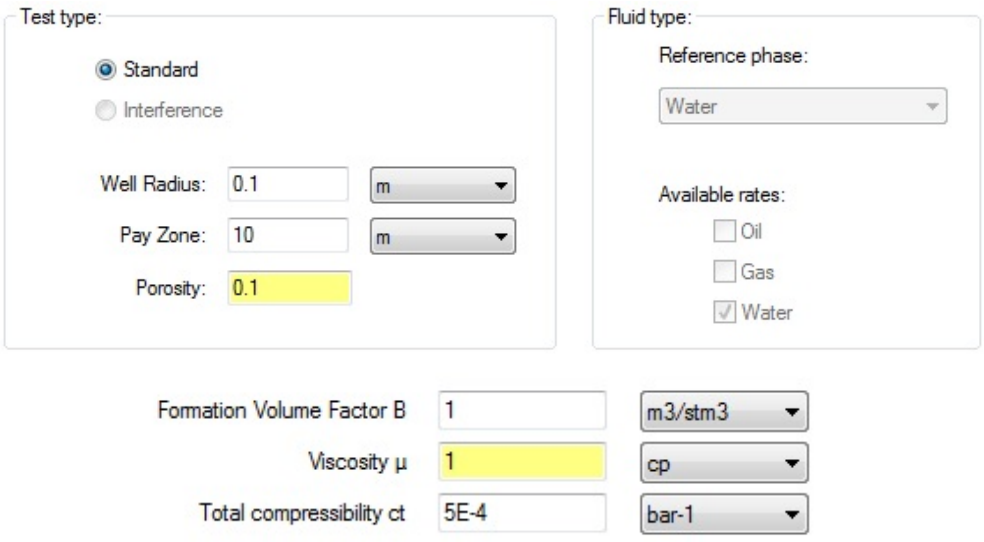

Figure 4.1: Well & Reservoir initialization in SAPHIR (PTA tool)

In the PTA tool, well and reservoir parameters are set in i.e. well radius, total compressibility, viscosity of fluid and net thickness. Then bottom-hole pressure versus time values are taken from the simulation results (numerical) and loaded into the PTA tool, this includes the rates in the correct time periods (flowing/shut-in). After all necessary data are put in the PTA tool, we can extract the pressure and pressure derivative which is our numerical simulation result. The tool also provides the analytical model that needs to be adjusted according to the conditions specified in ECLIPSE. The adjustments include the boundary conditions and distance, the initial pressure, wellbore storage and the skin factor. A good match between the analytical and the numerical solution shows the compatibility of well-reservoir parameters with both solutions, giving a reliable interpretation of the reservoir properties i.e. the flow capacity (permeability).

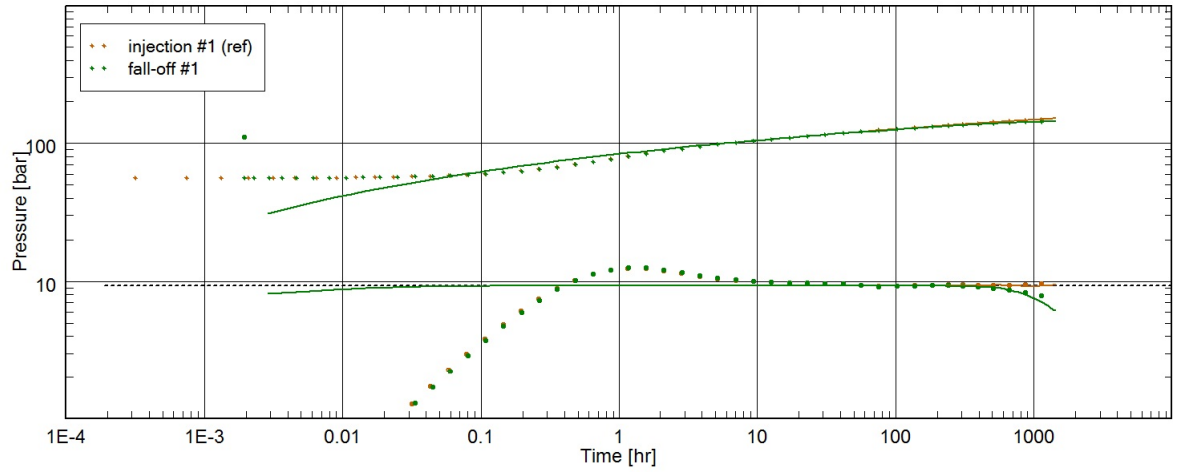

Figure 4.2: Numerical (dots) & Analytical (line), pressure and derivative response for Case 1.

Figure 4.2 shows results of the analytical and numerical match, of pressure and pressure derivative for the constant permeability case. It indicates an acceptable match between the analytical model (green/yellow line) and numerical simulation result (green/yellow dots) regarding the simulated case with constant flowing rate and non-pressure dependent permeability. A difference between the results may be due to a numerical error, which can be minimized by reducing the grid dimensions and time steps in the simulator. The result match approve the simulation model for constant permeability ($\gamma = 0$).

The figure below shows the injection and fall-off periods with the equivalent rates as used in the numerical simulation. The bottom-hole pressure versus time (green dots) is loaded into SAPHIR from ECLIPSE, and the matching analytical model is generated by SAPHIR (red line).

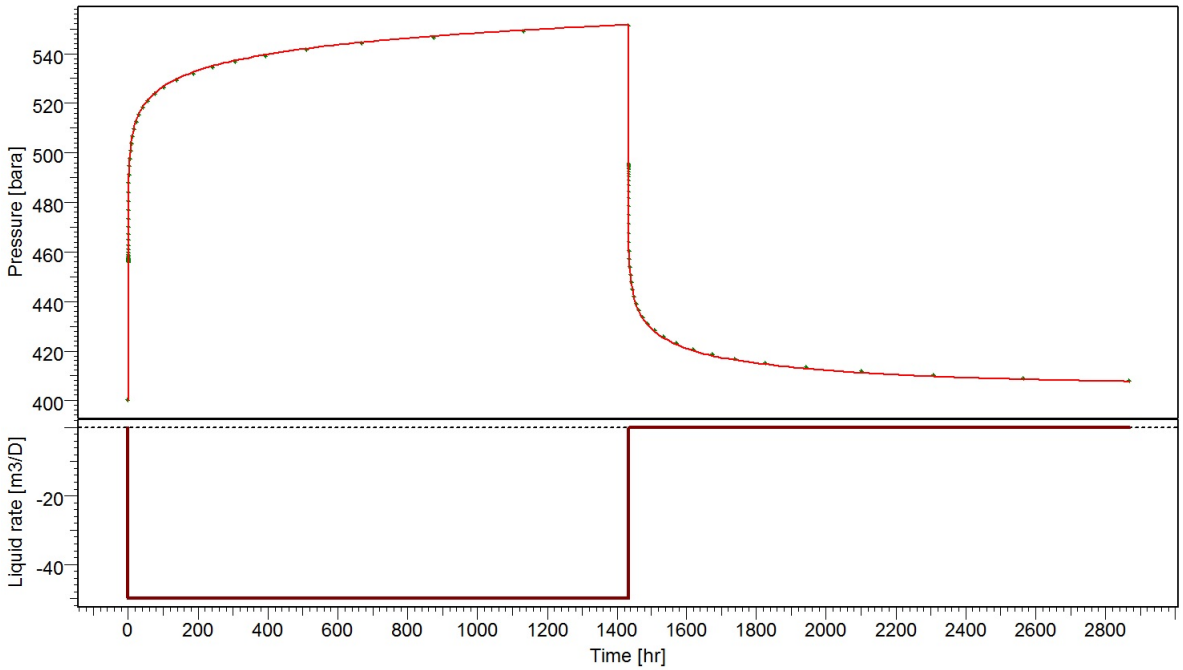

Figure 4.3: : Numerical (dots) & Analytical (line), Rate & Pressure vs Time for Case 1.

The match of the analytical model is obtained by calibrating it with the numerical result based on the two plots above and a semi-log plot. Different parameters are adjusted in the PTA tool in order to get the best match, these include; well, reservoir and boundary parameters i.e. boundary condition (no flow or constant pressure), distance to boundary, initial pressure and skin. Based on the analytical model match with the numerical simulation, the PTA tool provides the well-reservoir parameters, where permeability is the objective.

In this case we get a good match where the well-reservoir parameters inputted in simulation model are obtained from the PTA tool interpretation. This concludes that the method used for the numerical-analytical match is reliable.

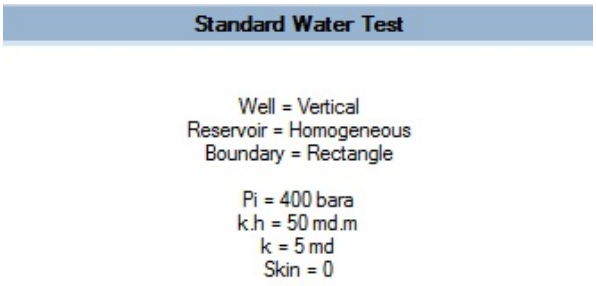

Figure 4.4: Permeability result from interpretation

4.2 Simulation of Step-Rate Test

In this section we present the method for step-rate test (SRT) in the simulation model and how to analyze it in the PTA tool. In the previous chapter (Reservoir Simulation Studies) a test consisting of one injection period and one fall-off period was implemented in our model, whereas in the following sections a different test is implemented. The step-rate test consists of multiple injection (flowing) periods with increasing rates and one fall-off (shut-in) period.

In the simulation model, different rate controls are set for each step (period) with equal time intervals for each flowing period. The SRT includes five injection periods with a time interval of 10 days (240 hours) each. This is followed by a shut-in period for 60 days (1440 hours). Table 3 includes the injection rates used for the two cases in the following sections. Figure 4.6 shows how the pressure in the simulated step-rate test looks like (green dots).

Steps	Rate (m3/day)		Time (days)
	k(p)	k(p) w/fracture	
Step 1	20	50	10
Step 2	40	100	10
Step 3	60	150	10
Step 4	80	200	10
Step 5	100	250	10
	0	0	60

Table 3: SRT rates and time periods

The higher rates for the pressure dependent permeability case with fracture are set to ensure the bottom-hole pressure reaches the same level as in the case with no fracture. This is due to lower bottom-hole pressure when a hydraulic fracture exists.

The SRT provides the pressure and the time interval for the specified rate, which allows us to extract the pressure change and pressure derivative curves for each step. An analysis in the PTA tool is made for each rate step, where the analytical model is matched with the numerical simulation values as explained in section 4.1. Hence, the step-rate test provides permeability values for each step, which may help in delivering good estimated values of the pressure dependent permeability. The permeability values for each step along with pressure points could be plotted to get the estimated k(p) curve, presenting the numerical simulation for k(p). This may serve as the inverse solution for k(p), when comparing it with the true k(p) we may find out the accuracy of SRT in identifying permeability pressure dependence.

4.3 Pressure Dependent Permeability

The step-rate test presented above is simulated using Case 3 model (section 3.1.3), where permeability is pressure dependent. However, following our understanding of grid block size effect and boundary conditions on the simulation model, some adjustments are made. Hence, a refined grid (1 m * 1 m) is used where the reservoir size doesn't change (1000 m^2) but the grid block size decreases. As a closed system (no flow boundary) may complicate the analysis, to eliminate or delay the boundary effects, constant pressure boundary condition is simulated. This is to minimize error and ensure that the simulation produces more accurate numerical results in order to further interpret it in the PTA tool.

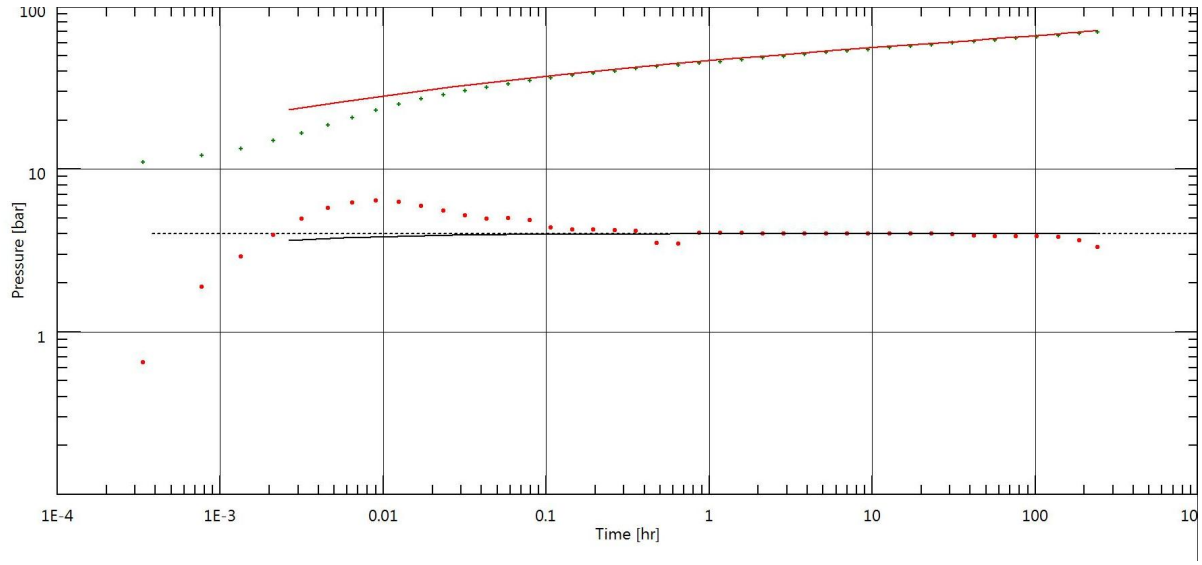

Figure 4.5: Step 2: Numerical (dots) & Analytical (line), pressure and derivative response for k(p) case.

The numerical results obtained from the simulation are supplied to the PTA tool. Following the same method as in section 4.1 we match the analytical model and numerical results in steps. For each rate step; the pressure and derivative responses for the analytical model are matched along with the well-reservoir parameters. The aim is to get a good analytical-numerical match in the PTA tool, to estimate permeability.

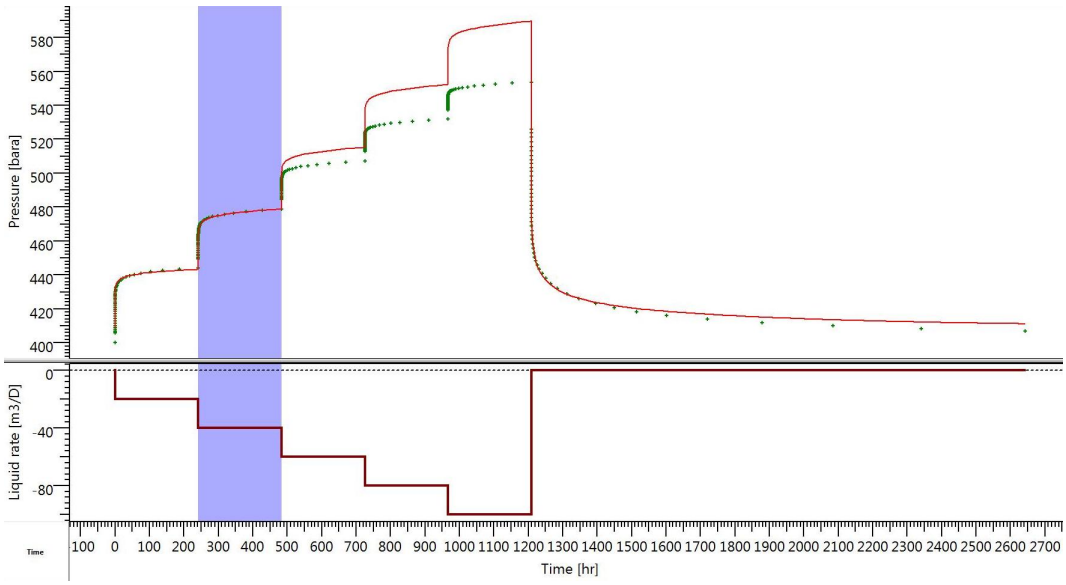

Figure 4.6: Analytical (red) & numerical (green) pressure match for step 2 of SRT, k(p).

For Step 2, figure 4.5 presents the pressure and pressure derivative for pressure dependent permeability case. This indicates a good match between the analytical model (black/red line) and numerical simulation (red/green dots) regarding step 2 with 40 m3/day rate. The match is supported with the history plot showing the pressure match for the models in figure 4.6. The same analysis is performed for step 5, presenting a good match in figure 4.7.

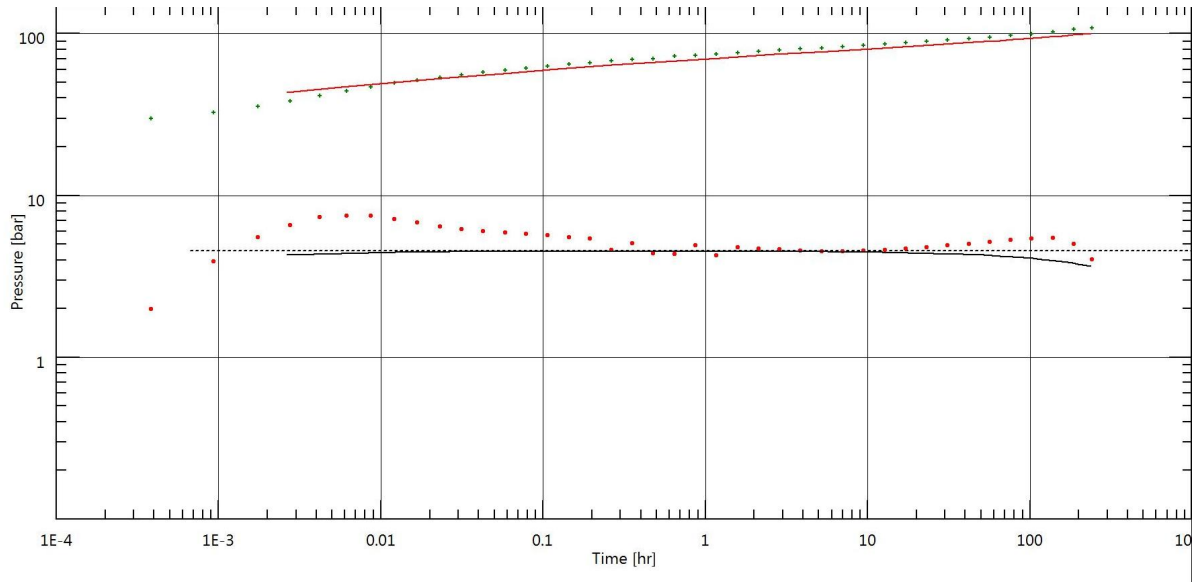

Figure 4.7: Step 5: Numerical (dots) & Analytical (line), pressure and derivative response for k(p) case.

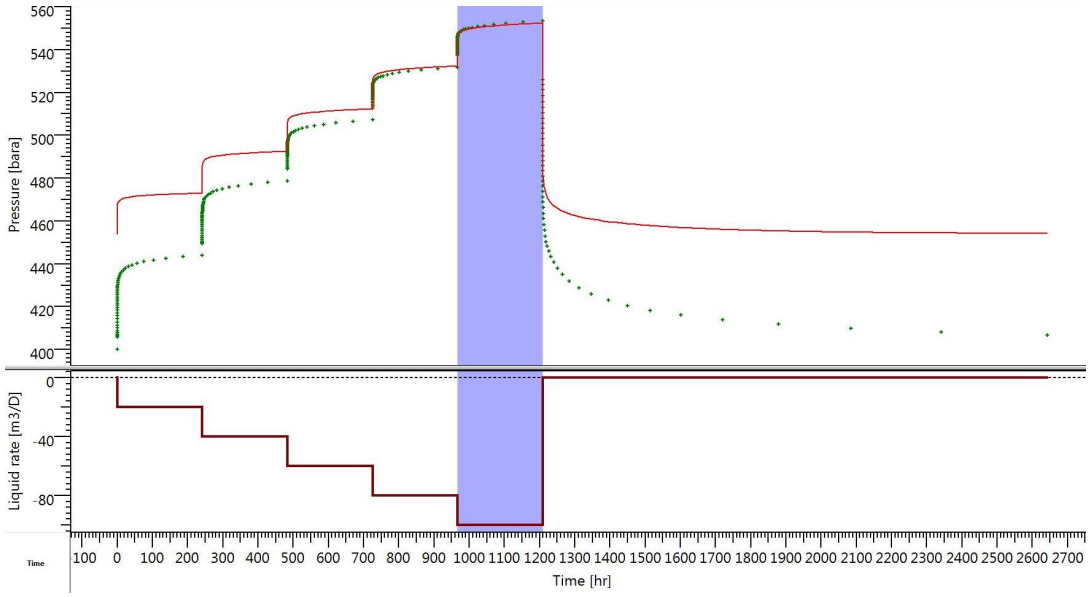

Figure 4.8: Analytical (red) & numerical (green) pressure match for step 5 in SRT, k(p).

The numerically simulated SRT response was analyzed using conventional interpretation of pressure transient at each step in order to get permeability estimate and to construct k(p) curve. The interpretation provided five permeability values, which are plotted against the highest pressure point of each step (figure 4.9). Now we can see the comparison between the estimated k(p) curve obtained through the inverse problem solution and the k(p) initially implemented in the numerical simulation.

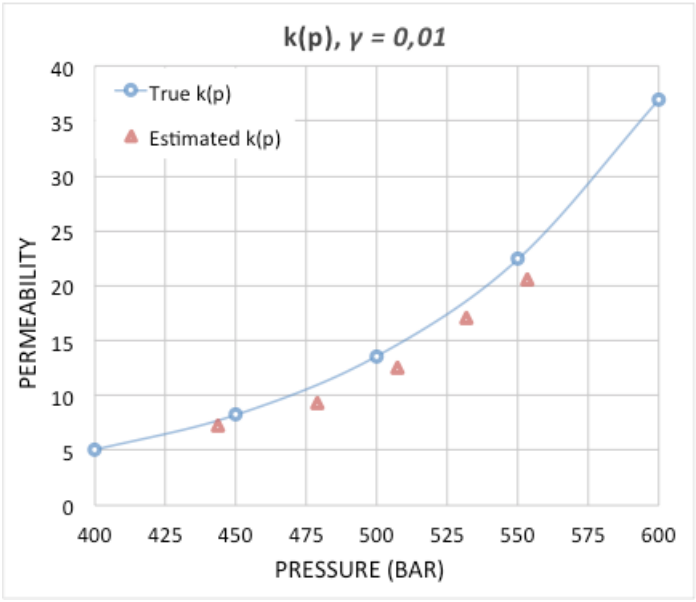

Figure 4.9: Comparison k(p)

The resulted permeability values are located near the true k(p) curve that confirmed acceptable quality of the estimation (figure 4.9). As it could be observed, the reference pressure for estimated values are 5-10% higher than the reference pressures in the initial curve (the points are below the true curve). This observation may be related to the difference

between the reservoir and bottom-hole pressures: the true curve relates permeability with reservoir pressure, while the estimated values relates it to the maximum well (bottom-hole) pressure.

It should be noted that the numerical simulation has numerical dispersion and analytical representation of well inflow through difference between well (bottom-hole) pressure and pressure in the grid block containing the well that may cause simulation errors, particularly in the case of pressure dependent permeability. This may affect the synthetic well test responses obtained from the simulation, which may cause uncertainty in the interpretation, e.g. artificial skin factor necessary to match the synthetic response (figure 4.10).

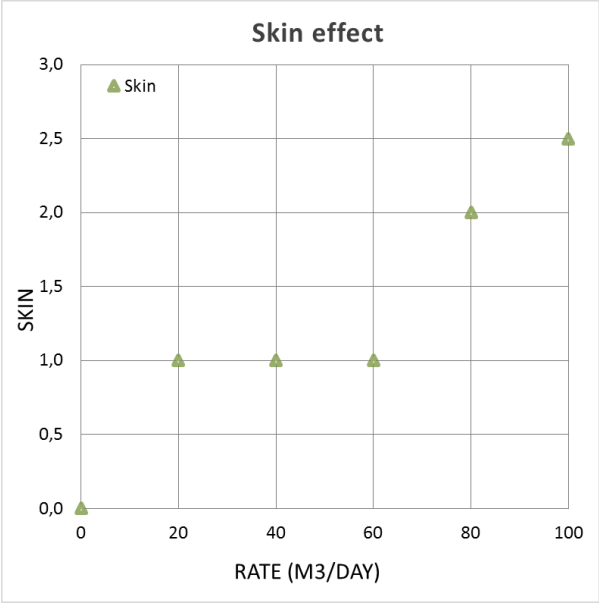

Figure 4.10: Skin effect

From the analysis preformed to match the numerical simulation response with the analytical model, we got a skin factor, which was not present in the numerical simulations (skin was zero). It is interesting that skin increases with higher rates (figure 4.10). This unusual effect appears only for the pressure dependent permeability model, in comparison with SRT for constant permeability model where there was no skin. Nonetheless, the skin effect does not significantly affect the permeability values obtained.

Simulation runs with fine grids did not eliminate this unusual skin. Due to the time limits of the study no more runs were carried out to examine this problem. However, it would be of interest to further investigate this effect to understand its reasons. Furthermore, we contemplate that a numerical error in the grid block to well connection develops when pressure dependent permeability is assumed in the model, mimicking the skin effect.

4.4 Pressure Dependent Permeability with Fracture

In this section we simulate a pressure-sensitive reservoir with a fracture, similar to case 4 (section 3.1.4), to study the effect a hydraulic fracture has on the estimated pressure dependent permeability. The same refined model as in section 4.3 was used, with an addition of a fracture extending from the well with a half-length of 25 meters. The analytical-numerical interpretation would provide the estimated permeability values necessary to build the k(p) curve.

Using the numerical simulation results, the well test is interpreted in the PTA tool. The well-reservoir parameters in SAPHIR were adjusted accordingly to match the simulated model (ECLIPSE). The 'infinite-conductivity fracture' well model was chosen as to generate the analytical models, and the half-length was specified for all the steps. Constant pressure boundary and distance to the boundary were also modified as done in the previous interpretation.

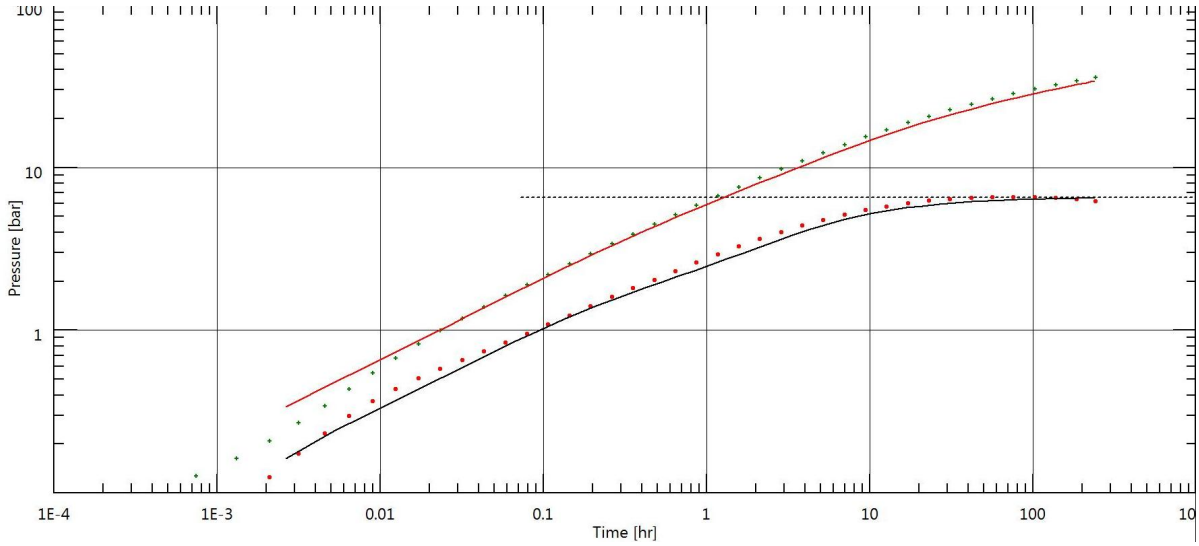

Figure 4.11: Step 1: Numerical (dots) & Analytical (line), pressure and derivative response for k(p) with fracture.

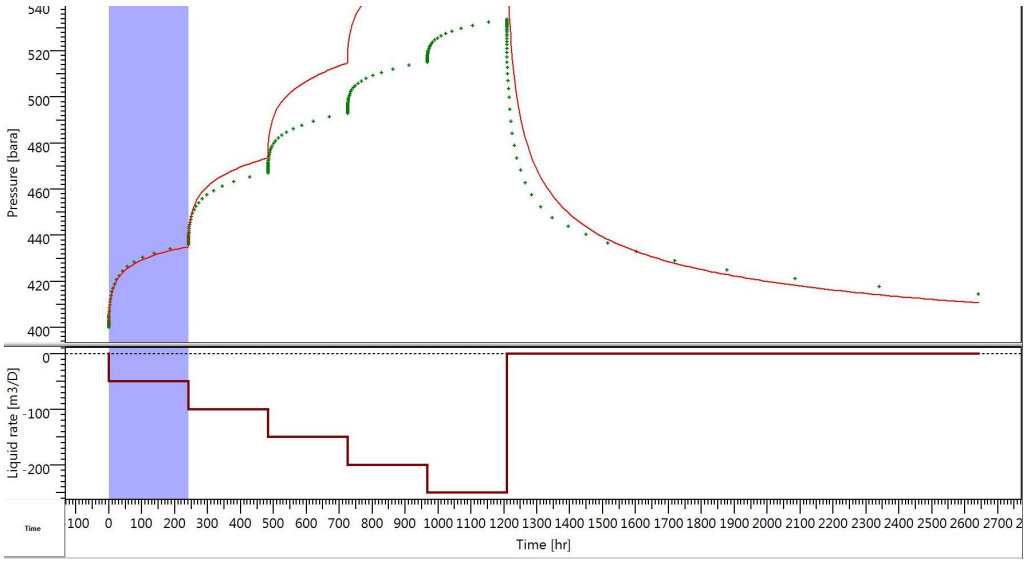

Figure 4.12: Analytical (red) & numerical (green) pressure match for step 1, k(p) with fracture.

Figure 4.11 above presents the analytical-numerical match for Step 1. The linear flow regime for an infinite conductive fracture from the numerical simulation results is presented by the pressure derivative, also matched with the analytical model. The dotted horizontal line helps to present the radial flow regime, which is used to estimate the permeability. The history plot (figure 4.12) presents the pressure match for step 1 which supports the interpretation. Here the flow rate for step 1 was set to 50 m3/day increasing to 250 m3/day for step 5, as the pressure increase in the well is lower in presence of hydraulic fracture.

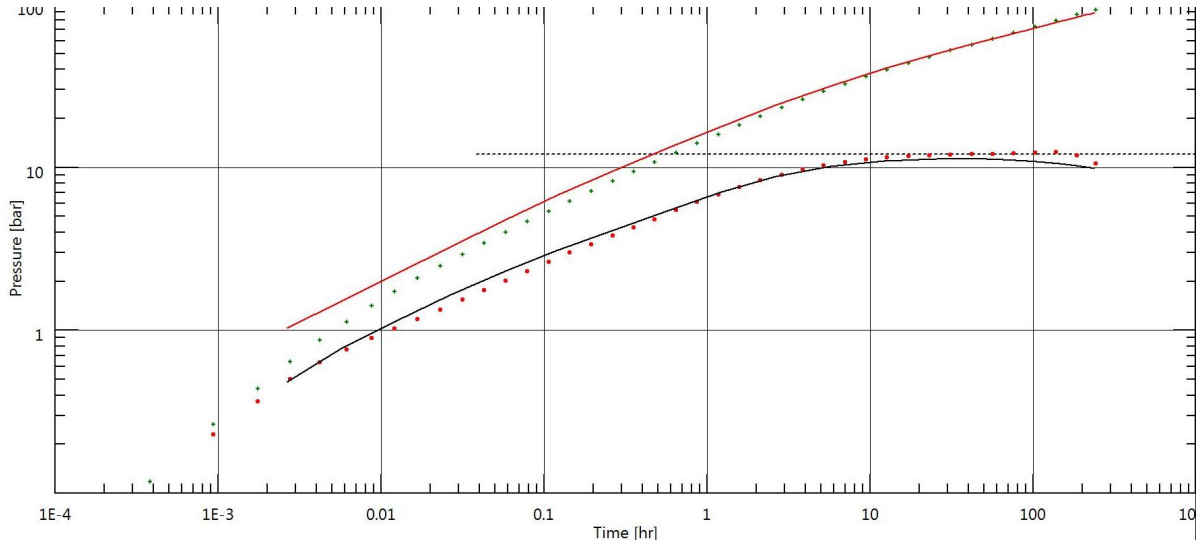

Figure 4.13: Step 5: Numerical (dots) & Analytical (line), pressure and derivative response for k(p) for fracture.

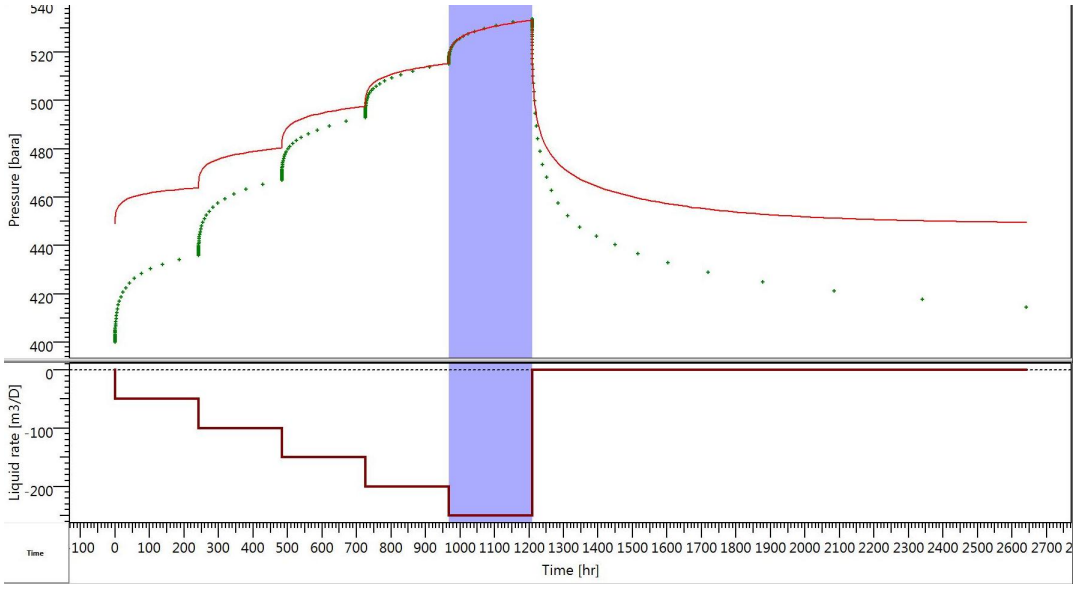

Figure 4.14: Analytical (red) & numerical (green) pressure match for step 5, k(p) with fracture.

The interpretation for Step 5 is shown in figure 4.13. The analysis for all the steps was preformed. We notice that the analytical models generated by the PTA tool have a very good match with the simulated results at a chosen step. In the reservoir simulation the fracture acts as a constant pressure boundary. Moreover there was no skin effect observed, due to the presence of fracture (constant pressure boundary), reducing the interpretation uncertainty.

The analytical model from the PTA tool presents a reliable solution to estimate pressure dependent permeability using step-rate test. Each permeability value is associated with the highest pressure point of each step.

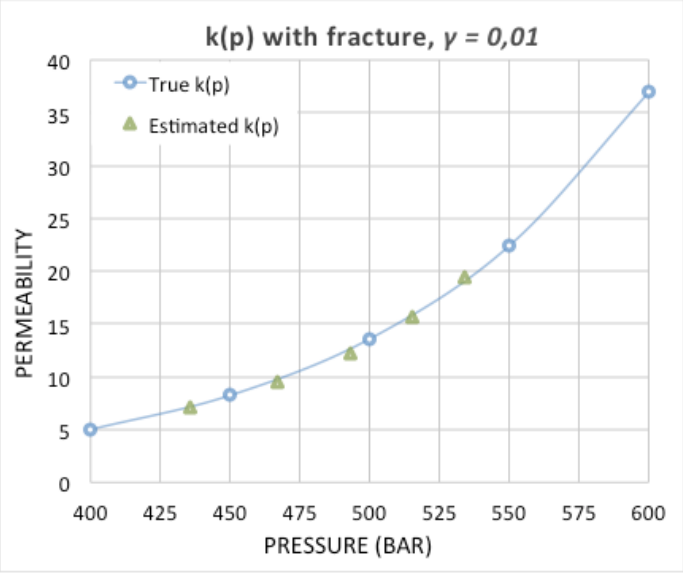

Figure 4.15: Comparison of k(p) with fracture

The estimated permeability values accurately match the initially specified (true) k(p) curve (figure 4.15). This confirmed the capability of the analytical model of interpreting k(p) function from step-rate test analysis.

From the simulation perspective, the well grid block lies in the middle of the fracture grid blocks where pressure is uniform (refer section 3.2.1), this conducts the pressure in the bottom-hole (well) to pressure in the reservoir (near wellbore). Hence, the alignment of the true and estimated k(p) curves in figure 4.15 provides quiet an accurate result.

4.5 Conclusion of Well Test Interpretation

In this chapter we presented the interpretation of synthetic well tests responses obtained from numerical simulations with analytical models generated by PTA tool. Well test response from the simulated step-rate test provides permeability values for each step, which delivers good estimated values of pressure dependent permeability. The estimated (interpreted) k(p) values are compared to the true (specified) k(p) values to discover the capability of the interpretation method.

Based on the analytical-numerical interpretation, some conclusions were made:

- The method used for the numerical-analytical interpretation is reliable. (section 4.1)
- Estimating the k(p) curve through inverse problem solution may present capability of interpreting well tests to find true k(p).
- Reference (bottom-hole) pressures for the estimated k(p) seem to be 5-10% higher than the reference (reservoir) pressures in the true k(p) curve (figure 4.9).
- Possible simulation error in the grid block to well connection may develop when pressure dependent permeability is assumed in the model, mimicking a skin effect (figure 4.10).
- Presence of infinite-conductivity fracture (i.e. constant pressure boundary) can reduce uncertainty in the interpretation (figure 4.15)
- The match between permeability estimated values and the initially specified (true) k(p) curve shows the capability of interpreting k(p) function from step-rate test.

5 Results and Conclusions

In the study, we have numerically investigated well test responses of reservoirs with pressure dependent permeability in comparison to constant permeability. This dynamic permeability was used in the simulations and cases with an induced fracture were also simulated. The segment reservoir model provided synthetic well test responses, which were interpreted with the analytical model usually used in well test interpretation. Thus, we were able to estimate the function k(p), which corresponded to the function k(p) initially specified in the simulations, i.e. estimated k(p) curve was in agreement with the true function k(p).

Based upon results from the work performed the following conclusions were may be drawn:

- If pressure dependent permeability k(p) is neglected, inaccurate values of permeability may be estimated from pressure transient analysis.
- Injection period for k(p) case gives higher flow capacity (kh) than the initial kh for the constant permeability case.
- It appears like pressure dependent permeability does not impact the linear flow to the induced fracture.
- The step-rate tests simulated yielded reliable pressure transients for detecting and estimating k(p).
- Analytical models from the well test interpretation software are capable of interpreting k(p), if step-by-step interpretation of pressure transients is applied.
- Analytically interpreted k(p) may vary from the initially specified k(p) that may be related to inaccuracy of the near wellbore numerical simulation in the case of pressure sensitive.
- Permeability modulus (γ) can be estimated from step-rate test data using conventional interpretation techniques.

For the cases analyzed in chapter 4, an adequate match was obtained combining the analytical model and the numerical simulation. Both analytical models with and without a fracture provided reasonable estimations of k(p). However, in the case without fracture there was 5-10% difference observed between the numerical and analytical bottom-hole, which was matched in the analytical model using well skin factor (not present in the numerical simulations). This effect may be related to the analytical calculation of well inflow in the numerical simulation that could lead to inaccurate pressure simulation in the near wellbore area for the case of pressure sensitive reservoirs. This effect was not studied in the thesis and may be addressed in a special study. The presence of high conductivity fracture (similar to

constant pressure boundary) helped to reduce the observed pressure difference providing reliable interpretation of k(p) without artificial skin. This confirmed the capability of the analytical models in interpreting k(p) from step-rate tests of actual wells.

6 References

Al Hussainy R., Ramey H. and Crawford P., *The Flow of Real Gases Through Porous Media,* Journal of Petroleum Technology, Volume 18, Number 5, pp. 624-636, May, 1966.

Arevalo-Villagran, J. A., Cinco-Ley, H., Wattenbarger, R. A., Garcia-Hernandez, F., & Samaniego-Verduzco, F. (2003, January 1). *Transient Analysis of Tight Gas Well Performance - More Case Histories*. SPE 84476-MS

Chin, L. Y., Raghavan, R., & Thomas, L. K. (2000, March 1). *Fully Coupled Geomechanics and Fluid-Flow Analysis of Wells With Stress-Dependent Permeability*. SPE 58968-PA

Cesar Alexander Rodriguez, 2004. *Stress-Dependent Permeability on Tight Gas Reservoirs*. Master Thesis, Texas A&M University.

Dominique Bourdet. (2002). *Well Test Analysis - The Use of Advanced Interpretation Models*.

Fluid flow in hydraulically fractured wells. (2015). Retrieved from petrowiki.org: *http://petrowiki.org/Fluid_flow_in_hydraulically_fractured_wells*

Franquet, M., Ibrahim, M., Wattenbarger, R. A., & Maggard, J. B. 2004. *Effect of Pressure-Dependent Permeability in Tight Gas Reservoirs, Transient Radial Flow*. Petroleum Society of Canada. PETSOC-2004-089.

Gringarten, A. C., Ramey, H. J., & Raghavan, R. (1974, August 1). *Unsteady-State Pressure Distributions Created by a Well With a Single Infinite-Conductivity Vertical Fracture*. SPE 4051-PA.

Kikani, J., & Pedrosa, O. A. (1991, September 1). *Perturbation Analysis of Stress-Sensitive Reservoirs* (includes associated papers 25281 and 25292). SPE 20053-PA

Laura Maria Priskila, 2014. *Evaluation of Fishbone Lateral Stimulation*. Master Thesis, Norwegian University of Science and Technology.

Mariela Franquet Barbara, 2004. *Effect of Pressure-Dependent Permeability on Tight Gas Wells*. Master Thesis, Texas A&M University.

Okbit Berhe, 2014. *Correct sampling of gas condensate reservoir with liquid drop around the well*. Master Thesis, University of Stavanger.

Pattay, P. W. (1998, January 1). *Transient Pressure Behavior in Fractured Reservoirs. Society of Petroleum Engineers*. SPE 52080-STU.

Pedrosa, O. A. (1986, January 1). *Pressure Transient Response in Stress-Sensitive Formations*. SPE 15115-MS.

Pinzon, C. L., Chen, H.-Y., & Teufel, L. W. (2001, January 1). *Numerical Well Test Analysis of Stress-Sensitive Reservoirs.* SPE 71034-MS.

Qanbari, F., & Clarkson, C. R. 2014. *Analysis of Transient Linear Flow in Stress-Sensitive Formations*. SPE 162741-PA.

Raghavan, R., Scorer, J. D. T., & Miller, F. G. (1972, June 1). *An Investigation by Numerical Methods of the Effect of Pressure-Dependent Rock and Fluid Properties on Well Flow Tests.* SPE 2617-PA

Raghavan, R., & Chin, L. Y. (2004, August 1). *Productivity Changes in Reservoirs With Stress-Dependent Permeability*. SPE 88870-PA

Reservoir flow. (2015). Retrieved from fekete.com: *http://www.fekete.com/SAN/WebHelp/FeketeHarmony/Harmony_WebHelp/Content/HTML_Files/Reference_Material/General_Concepts/Reservoir_Flow.htm*

Samaniego V., F., Brigham, W. E., & Miller, F. G. (1977, April 1). *An Investigation of Transient Flow of Reservoir Fluids Considering Pressure-Dependent Rock and Fluid Properties.* SPE 5593-PA

Samaniego, F., & Cinco-Ley, H. (1989, January 1). *On the Determination of the Pressure-Dependent Characteristics of a Reservoir Through Transient Pressure Testing*. SPE 19774-MS

Shchipanov, A., Berenblyum, R., & Kollbotn, L. (2014, October 27). *Pressure Transient Analysis as an Element of Permanent Reservoir Monitoring*. SPE 170740-MS.

Shchipanov, A., Kollbotn, L., Berenblyum, R., & Surguchev, L.M. (2011). *How to Account for Dynamic Fracture Behaviour in Reservoir Simulation.* EAGE-NHF27.

U.S. EPA, Region VI, 2002. *UIC Pressure Falloff Testing Guideline, Third Revision*.

Well test theory and equations. (2015). Retrieved from fekete.com: *http://www.fekete.com/SAN/TheoryAndEquations/WellTestTheoryEquations/*

Yale, D. P., & Nur, A. (1985, January 1). *Network Modeling of Flow, Storage, And Deformation In Porous Rocks*. Society of Exploration Geophysicists.

Zhang, M. Y., & Ambastha, A. K. (1994, January 1). *New Insights in Pressure-Transient Analysis for Stress-Sensitive Reservoirs.* SPE 28420-MS.

7 Nomenclature

A Reservoir drainage area, m^2 *or* ft^2

h Reservoir thickness, m *or* ft

k Permeability, md

k_i Initial permeability, md

$k(p)$ Pressure dependent permeability, md

Q Flow rate, Sm^3/day

γ_p Permeability modulus parameter

μ_o Viscosity of oil, cP

B_o Oil formation volume factor, Sm^3/Sm^3

$\emptyset$ Porosity

c_t Total compressibility, bar^{-1} *or* $psia^{-1}$

s Skin factor

t_D Dimensionless time

P Pressure, $bars$ *or* $psia$

p_i Initial pressure, $bars$ *or* $psia$

P_D Dimensionless pressure

p'_D Dimensionless pressure derivative

$m(p)$ Real gas pseudo-pressure, $psia^2/cP$

Z Compressibility factor

Abbreviations

PTA Pressure Transient Analysis

BHP Bottom Hole Pressure, *psia or bars*

PSS Pseudo Steady State

SS Steady State

FO Fall-Off period

INJ Injection period

SRT Step Rate Test

md milli darcy (permeability unit)

8 Appendix

Appendix A – Eclipse model

The ECLIPSE model below was used to simulate constant permeability and pressure dependent permeability, for Chapter 3. This represents the base case model which was also used for simulations in Chapter 4. However, some adjustments were made like refining the grid dimensions, including multiple injection rate periods (SRT) etc.

```
--Pressure-Dependent Permeability for Single-Phase model.
--By Mahmoud Alaassar
RUNSPEC    ======================
TITLE
  Injection + Fall-off, Injector Simulation
DIMENS
   101   101   1 /
OIL
WATER
METRIC
WELLDIMS
   10   10   2   2 /
NOECHO
ROCKCOMP
 REVERS  2  /  to apply k(p)
START
  1 'FEB' 2015  /
UNIFOUT
UNIFIN

GRID    =========================
INIT
NOECHO
DX
```

```
 10201*10 /
DY
 10201*10 /
DZ
 10201*10 /
PERMX
 10201*5 /
PERMY
 10201*5 /
PERMZ
 10201*5 /
PORO
 10201*0.1 /
TOPS
 10201*2000 /
--ACTIVATE BOX, PERMX TO IMPLEMENT FRACTURE
--BOX
 --46 56  51 51  1 1 / (11-blocks) fracture length
PERMX
 11*500000 /
ENDBOX
--ACTIVATE BOX & PORO TO IMPLEMENT CONSTANT PRESSURE BOUNDARY
--BOX
--  1   2   1  101   1  1  /
--PORO
-- 202*1.0D6 /
--BOX
-- 100 101  1  101   1  1 /
--PORO
 --202*1.0D6 /
--BOX
```

```
-- 1 101 1 2 1 1 /
--PORO
--202*1.0D6 /
--BOX
-- 1 101 100 101 1 1 /
--PORO
--202*1.0D6 /
--ENDBOX
RPTGRID
/

PROPS ============================
NOECHO
-- ACTIVATE RKTRMDIR & ROCKTAB TO IMPLEMENT PRESSURE DEPENDENT PERMEABILITY
RKTRMDIR
--permeability modulus of 0.01
ROCKTAB
-- Pressure PV multi TransX TransY TransZ
  50        0.84       0.03     0.03     1
  100       0.86       0.05     0.05     1
  150       0.88       0.08     0.08     1
  200       0.90       0.14     0.14     1
  250       0.93       0.22     0.22     1
  300       0.95       0.37     0.37     1
  350       0.98       0.61     0.61     1
  400       1          1.00     1.00     1
  450       1.03       1.65     1.65     1
  500       1.05       2.72     2.72     1
  550       1.08       4.48     4.48     1
  600       1.11       7.39     7.39     1
  650       1.13       12.18    12.18    1
```

```
   700          1.16          20.09     20.09     1
   750          1.19          33.12     33.12     1
   800          1.22          54.60     54.60     1
   850          1.25          90.02     90.02     1
   900          1.28          148.41    148.41    1
   950          1.32          244.69    244.69    1
  1000          1.35          403.43    403.43    1  /
/
SWOF
 0 0 1 0
 1 1 0 0
/
PVTW
 400  1   0   1   0  /
PVCDO
 400  1   0  0.5  0 /
--TO BE DEACTIVATED WHEN ROCKCOMP/ROCKTAB ARE USED
--ROCK
-- 400    5.0D-4   /
DENSITY
  830   1025   0.8  /

SOLUTION   ==========================
PRESSURE
 10201*400 /
SWAT
 10201*1 /
RPTSOL
  'RESTART=2' /
RPTRST
 'BASIC=6' ROCKC /
```

```
SUMMARY   ============================
NOECHO
EXCEL
DATE
FWPR
FWCT
WBHP
'INJE' /
FWIR

SCHEDULE   ============================
RPTSCHED
 'RESTART=2' /
WELSPECS
 'INJE'  'G'  51  51  1*  'WATER'/
 /
COMPDAT
 'INJE'   51  51  1 1  'OPEN'  2*  0.2  /
 /
-- FLOWING & SHUT-IN PERIODS, more periods for SRT.
-- INJECTION WELL CONTROLS
-- THE INJECTION RATE IS CONTROLLED HERE, multiple rates for SRT
-- CONSTANT FLOW RATE.
--INJECTION RATE, 50 rm3/day (varies with SRT)
WCONINJ
 'INJE'  'WATER'  'OPEN' 'RATE' 50 3* /
 /

TSTEP
1.3250380e-05 1.7853104e-05 2.4054656e-05 3.2410414e-05 4.3668673e-05
```

5.8837662e-05 7.9275835e-05 1.0681352e-04 1.4391685e-04 1.9390860e-04

2.6126576e-04 3.5202046e-04 4.7430022e-04 6.3905574e-04 8.6104165e-04

1.1601378e-03 1.5631296e-03 2.1061069e-03 2.8376957e-03 3.8234133e-03

5.1515350e-03 6.9410005e-03 9.3520645e-03 1.2600649e-02 1.6977679e-02

2.2875139e-02 3.0821173e-02 4.1527384e-02 5.5952564e-02 7.5388553e-02

1.0157593e-01 1.3685991e-01 1.8440032e-01 2.4845462e-01 3.3475918e-01

4.5104296e-01 6.0771971e-01 8.1882057e-01 1.1032506e+00 1.4864817e+00

2.0028342e+00 2.30416667e+00 2.6985496e+00 3.6359326e+00 4.8989301e+00

6.5869482e+00 8.5847382e+00 10.6839485e+00 12.5749392e+00 /

WELSPECS

'INJE' 'G' 51 51 1* 'WATER'/

/

WCONINJ

'INJE' 'WATER' 'STOP' 'RATE' 50 3* /

/

TSTEP

1.3250380e-05 1.7853104e-05 2.4054656e-05 3.2410414e-05 4.3668673e-05

5.8837662e-05 7.9275835e-05 1.0681352e-04 1.4391685e-04 1.9390860e-04

2.6126576e-04 3.5202046e-04 4.7430022e-04 6.3905574e-04 8.6104165e-04

1.1601378e-03 1.5631296e-03 2.1061069e-03 2.8376957e-03 3.8234133e-03

5.1515350e-03 6.9410005e-03 9.3520645e-03 1.2600649e-02 1.6977679e-02

2.2875139e-02 3.0821173e-02 4.1527384e-02 5.5952564e-02 7.5388553e-02

1.0157593e-01 1.3685991e-01 1.8440032e-01 2.4845462e-01 3.3475918e-01

4.5104296e-01 6.0771971e-01 8.1882057e-01 1.1032506e+00 1.4864817e+00

2.0028342e+00 2.30416667e+00 2.6985496e+00 3.6359326e+00 4.8989301e+00

6.5869482e+00 8.5847382e+00 10.6839485e+00 12.5749392e+00 /

END